Algal Research 68 (2022) 102890

Contents lists available at ScienceDirect

Algal Research

journal homepage: www.elsevier.com/locate/algal

Interactive effects of solar radiation and inorganic nutrients on biofiltration, biomass production, photosynthetic activity and the accumulation of bioactive compounds in *Gracilaria cornea* (Rhodophyta)

Félix L. Figueroa [a,*], Félix Álvarez-Gómez [a], José Bonomi-Barufi [b], Julia Vega [a], Thais F. Massocato [b], Juan Luis Gómez-Pinchetti [c], Nathalie Korbee [a]

[a] Universidad de Málaga, Instituto andaluz de Biotecnología y Desarrollo Azul (IBYDA), Departamento de Ecología y Geología, Campus Universitario de Teatinos s/n, 29071 Málaga, Spain
[b] Botany Department, Federal University of Santa Catarina, Campus of Trindade, Florianópolis, 88040-970, Santa Catarina, Brazil
[c] Spanish Bank of Algae, Institute of Oceanography and Global Change (IOCAG), University of Las Palmas de G.C., Muelle de Taliarte s/n, 35214 Telde, Canary Islands, Spain

ARTICLE INFO

Keywords:
Biomass productivity
Biofiltration
Gracilaria cornea
In vivo chlorophyll *a* fluorescence
Mycosporine-like amino acids
Nutrients
Tank culture

ABSTRACT

Interactive effects of solar radiation and inorganic nitrogen and phosphate on biofiltration capacity, biomass production, photosynthetic activity and the accumulation of bio-active compounds were studied in the red alga *Gracilaria cornea* grown in tanks with a seawater open-flow system during 35 days. Two light conditions were utilized: outdoor (O), full solar natural radiation, and indoor, inside of a greenhouse (G) where UV-B radiation was cut-off and part of the UV-A radiation was filtered. Two inorganic nitrogen and phosphate concentrations were used: High nutrients (HN; 100–200μM of NH_4^+ and 20μM of $KHPO_4$) and Low nutrients (LN; 10–20μM of NH_4^+ and 1μM of $KHPO_4$). Growth and biomass productivity were related to the daily integrated electron transport rate determined *in situ*, as an estimator of daily photosynthetic activity. Nitrogen uptake efficiency (NUE) was close to 100 % under LN, whereas under HN it ranged from 50 to 70 % in the first week of culture, decreasing to 10–15 % in the rest of the experimental period. Nitrogen uptake rate (NUR) ranged from 20 to 45 mmol N m^{-2} h^{-1} under HN, and 5 to 18 mmol N m^{-2} h^{-1} in LN treatments. Morphological and pigmentation changes were evident through the culture period. The thalli under HN were more reddish under the indoor treatments, than that in LN. The internal compounds increased throughout the experimental period. Mycosporine-like amino acids (MAAs) were accumulated under HN. N plays a photoprotective role due to both the increased photosynthesis and the MAA content. Maximal MAA productivity reached 113–253 mg MAAs m^{-2} d^{-1} under the O-HN treatment, the highest level reported until now in the bibliography. *G. cornea* could be used for bioremediation of high N content waters. In addition, under full solar radiation and high N availability produce high levels of bioactive compounds as MAAs, polyphenols and biliproteins for cosmeceutical applications.

1. Introduction

In recent decades, anthropogenic activity has caused serious social, economic, and environmental problems on aquatic ecosystems [1]. The inadequate discharges of sewage and industrial wastewater and no treated effluents from aquaculture have led to the contamination of continental and coastal water resources, which has impacted aquatic ecosystems in several ways [1–3]. Eutrophication, habitat modification, changes in biodiversity, and loss of ocean ecosystem services are some examples of negative consequences due to anthropogenic activity on coastal areas [4–6]. Exploring and developing sustainable management practices to minimize the flux of waste and pollutants offshore can further protect marine ecosystems.

In order to reduce environmental impacts and optimize production, the aquaculture industry has been developing sustainable ways to cultivate marine organisms, including macroalgae [7,8]. Integrated multi-trophic aquaculture (IMTA) is an increasingly used practice that aims to cultivate organisms from different trophic levels in a single

* Corresponding author.
E-mail address: felixlfigueroa@uma.es (F.L. Figueroa).

https://doi.org/10.1016/j.algal.2022.102890
Received 22 March 2022; Received in revised form 10 August 2022; Accepted 27 October 2022
Available online 8 November 2022
2211-9264/© 2022 The Author(s). Published by Elsevier B.V. This is an open access article under the CC BY-NC-ND license (http://creativecommons.org/licenses/by-nc-nd/4.0/).

interconnected system [9–11]. IMTA systems promote sustainability by linking waste generated from fed aquaculture (*e.g.* finfish or shrimp) with organisms presenting biofiltration capacities (*e.g.*, nitrifying bacteria, seaweeds and shellfish) [7,12,13]. In this way, wastes become a resource, which reduces the discharge of nitrogen and phosphorus loads to coastal areas [14,15].

The use of algal biomass has increased over the years, including its application in food and agricultural industries, as well as in the energy, pharmaceutical and cosmetic sectors [16–19]. Algal biomass contains a variety of compounds with commercial interest, such as proteins, peptides, carbohydrates and lipids [20]. A recent study shows that the production of biomethane from macroalgae is very close to profitability [21]. Algae produce a wide range of secondary metabolites that provide additional health benefits, such as carotenoids, phenolic compounds, antioxidants, polyunsaturated fatty acids, and mycosporine-like amino acids (MAAs), among others, that have been successful in the market due to the increasing interest in consumption of natural products [22,23]. In the last few years, efforts have been made to provide consistent, safe and sustainable biomass through cultivation [8,24]. They have focused on understanding the environmental conditions that favor and optimize the production of algal compounds of interest to meet commercial requirements. In addition, the co-culture of different species under IMTA systems can enhance their growth or biochemical composition, as observed by Gao et al. [25]

The production of algal biocompounds is modulated by environmental factors, such as light and nutrients [26–28]. Variations in quality and quantity of light induces algal photoregulatory mechanisms related to the synthesis of biocompounds derived from secondary metabolism [29,30]. Under high ultraviolet radiation (UV-A and UV-B), algae can exhibit cellular photoprotection strategies that prevent cell damage *via* the synthesis of UV-absorbing compounds, such as MAAs in red algae [23,31,32]. Studies have investigated the use of UVR to induce and/or stimulate biocompounds derived from secondary metabolism, whose biological role in the photosynthetic organism is photoprotection and which have great potential to be applied in pharmaceutical and cosmeceutical sectors [33–35].

Nutrients, mainly nitrogen (N) and phosphorus (P), are one of the main limiting factors of algal growth and also constitute a potential role on photosynthesis, growth and synthesis of bioactive compounds [36–39]. Availability of nutrients in the medium also affects the production of secondary compounds in algae [15,40,41]. The inorganic nitrogen is fundamental for biosynthesis of proteins and pigments, including molecules involved in mechanisms of cellular repair [34,42,43]. Due to this, an increase of nitrate, nitrite and ammonium in algal-culture systems could promote growth rates and stimulation of secondary metabolism [44,45]. A positive relationship between nitrogen availability and accumulation of photoprotective N-compounds have been reported in different species of seaweeds [33,43,46]. Nitrogen availability could potentially increase algal resistance to high irradiance resulting from the activation of photoprotective mechanisms, such as synthesis of UV- absorbing compounds like MAAs [47,48]. Under nutrient enrichment aquaculture, such as IMTA systems, several above cited biocompounds are accumulated, *e.g.* MAAs, polyphenols or biliproteins for cosmeceutical uses [40,49], algal meal for feed in aquaculture [50–54], human food [17,55] or biostimulants for plants in agriculture [56,57]. Therefore, seaweed-filtered mariculture systems prevent the emission of effluents with high N and P-compounds and also act as a resource of algal-biomass containing valuable compounds [58,59].

In order to better understand algal metabolism and conditions that optimize the production of algal compounds under nutrient biofiltration scenarios, research has been carried out to analyze interactive effects between irradiance, light quality and inorganic nitrogen availability on growth rate, photosynthesis and accumulation of bioactive compounds with cosmeceutical properties in *Gracilaria* spp. as carotenoids, phycobiliproteins, polyphenols and MAAs [60,61]. Many studies conducted under laboratory conditions confirm the combined effects of inorganic nitrogen and UVR on the biosynthesis and accumulation of nitrogenous compounds related to algal photoprotection [33,43,47,48]. Korbee et al. [46] reported that nitrogen supply with enriched ammonium seawater has a positive effect on MAAs accumulation in two *Porphyra* species. The effect of UVR on growth, photosynthesis, and accumulation of bioactive compounds under high ammonium supply in *Hydropuntia cornea*, *Gracilariopsis longissima* and *Halopithys incurva* has been also demonstrated [62].

Even though very few studies focused on outdoor system, many of them have reported the capacity of seaweed to reduce nutrient concentrations in fishpond effluents and other nitrogen sources, to convert in the process large quantities of nutrients into useful seaweed biomass [34,40,63,64]. Seasonal effects on the accumulation of MAAs or phenolic compounds were analyzed under the influence of solar radiation and nitrogen supply [61,65], or comparing the accumulation pattern in days with normal level of ozone *versus* days with low level of ozone related to an increase of UV-B radiation [66].

Success of coupling environmental conditions and algal physiology is relevant to optimize mass algal cultures and production of biocompounds. In this sense, the aim of the present research was to study interactive effects of radiation and nutrients on biofiltration, photosynthesis as *in vivo* chlorophyll *a* fluorescence, productivity, and biomass quality. The study was conducted by a bifactorial experiment in the red alga *Gracilaria cornea* cultivated in tanks at a pilot scale, simulating nitrogen and phosphate flow from fishpond effluents as it is the case of Integrated Multi-Trophic Systems compared to a control with low nutrient supply.

2. Material and methods

2.1. Biological material

Specimens of *Gracilaria cornea* J. Agardh (formerly *Hydropuntia cornea* (J.Agardh) M.J.Wynne; Guiry and Guiry, 2021) were obtained from stock cultures in the Spanish Bank of Algae (BEA) at Taliarte (east coast of Gran Canaria, Canary Islands, Spain) where it has been vegetatively cultivated during the last 30 years.

2.2. Experimental design

Pilot scale culture facilities at BEA were utilized in the experimental approach (Fig. 1), in which seawater is pumped from the sea, filtered and distributed through the pilot plant cultivation area. Enriched seawater with nutrients (N- and P- simulating fish-pond effluents) was distributed through the experimental tanks. Algae free-floating dynamic at the experimental tanks was obtained with the application of an open flow controlled turnover rates and forced aeration. Finally, seawater flows through a mangrove swamp with *Avicennia* sp. trees before being discarded.

G. cornea thalli were grown during 36 days in semi transparent cylindrical polyethylene tanks (94 L volume, 0.2 m^2 surface), receiving constant aeration through a bottom line. Four different treatments were analyzed (two radiation treatments and two nutrient concentrations). The algae were cultured under two light conditions: outdoor (O) with full solar natural radiation (PAR + UVR), and indoor inside a greenhouse (G) where UV-B ($\lambda = 280–320$ nm) radiation was cut-off and part of the solar UV-A radiation ($\lambda = 320–400$ nm) was filtered. The irradiance and temperature in both areas (O and G) were monitored during all the experiment using a radiometer data logger Zippo-HU12-PAR/UV (AO-electronics, Madrid, Spain). Temperature was followed using a HOBO U22 Water Temp Pro V.2 logger (Onset Computer Corporation, Massachusetts, USA). Nutrients were supplied through a continuous flow of seawater enriched in N and P (100-200 μM of NH_4Cl and 10-20 μM of $KHPO_4$). Nutrient turnover rates were 64 vol·day^{-1} (for the high nutrient treatment, HN) and 6.4 vol·day^{-1} (for the low nutrient

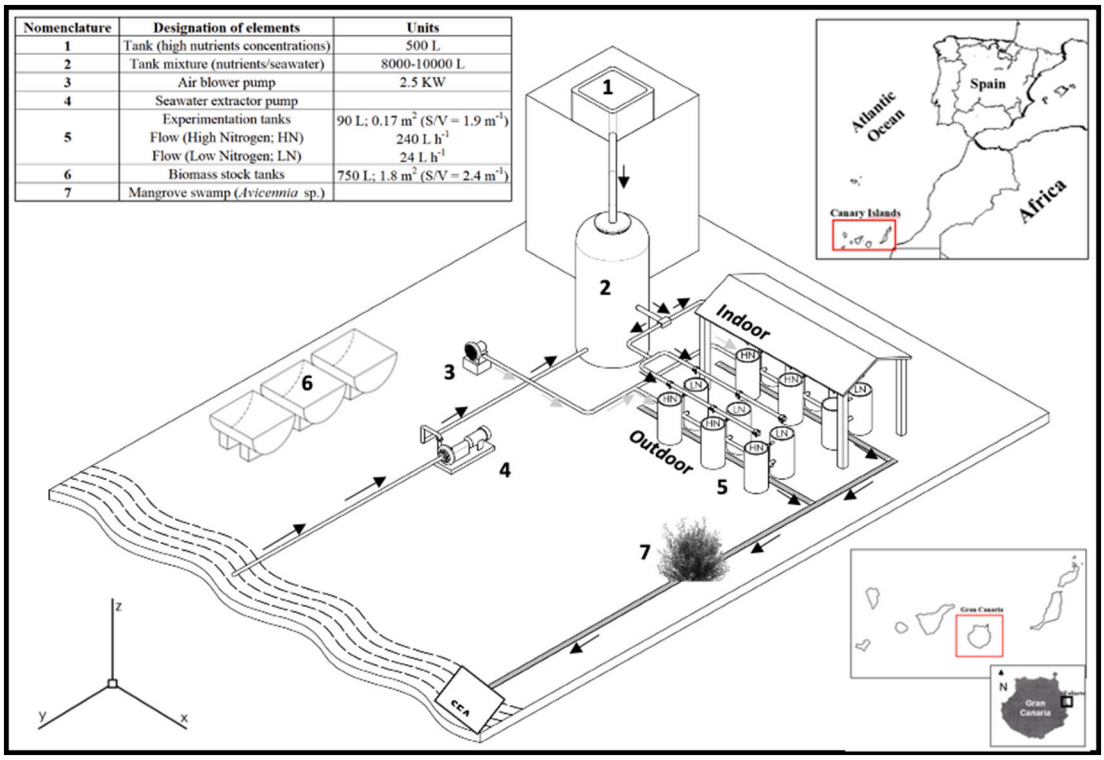

Fig. 1. Installation and experimental design using an isometric view of the open system at Spanish Bank of Algae (ULPGC) in Taliarte (Telde, Gran Canaria, Canary Islands, Spain: 28°00′N; 15°22′W). From the mother tank (1) in which N and P are added, the recirculation system is supplied through the mixing tank (2). Air injection by means of a blower pump (3), ensured homogeneous distribution and free algal biomass in the water column of the experimental tanks. The seawater was pumped (4) to the mixing tank. Each experimental unit containing 90 L of treated seawater (5) received the biomass of *Gracilaria cornea* from stock in nutrient-deprived conditions (6). The experimental units were kept indoor (in the greenhouse) and outdoor (in the full solar radiation) under controlled conditions for 35 days. The end of the system ends up returning to the sea, previously passing through a mangrove swamp of the *Avicennia* sp. trees, which ends up biofiltering nutrients (7).

treatment, LN).

2.3. Nitrogen biofiltration

Water samples were taken at 8, 15, 23, 28 and 35 days of experiment from the input and output of the tanks in order to determine the nitrogen uptake efficiency (NUE in %) and nitrogen uptake rate (NUR in μmol m^{-2} h^{-1}), using the following equations: NUE = 100-(C_2/C_1)·100 and NUR = F·(C_1-C_2)/A, where C_1 and C_2 are the concentration of NH_4^+ (μM) at the input and the output of the tanks, F is the flow rate ($L\ h^{-1}$), and A is the area of the tanks (m^2) [67].

Ammonium (NH_4^+) content was determined according to Parsons et al. [68]. 2.5 mL of the samples were mixed with 500 μL of phenol solution (100 mg mL^{-1} in distilled water), 500 μL of nitroprusiate solution (5 mg mL^{-1} in distilled water) and 1 mL of the oxidant solution (4:1 mixture of alkaline solution, *i.e.*, 200 mg sodium citrate and 10 mg NaOH and sodium hypochlorite solution at 1.5 N). The mixture was shaken and incubated in darkness and at room temperature for one hour. The absorbance of the reaction was determined spectrophotometrically at 640 nm by using UV-VIS 1700 Shimadzu spectrophotometer (Columbia, USA). Ammonium chloride was used as standard.

2.4. Growth rates and biomass productivity

At initial time, and after 7, 14, 21, 28 and 35 experimental days, the culture density was adjusted to 9 g fresh weight (FW) L^{-1}. Harvested biomass in different sampling days was weighted, frozen at −80 °C and freeze-dried (6.5 L Freeze Dryer, Labconco, USA). FW/DW ratio was calculated and used to estimate the accumulated dry biomass for each harvesting period. Growth rates were calculated for each period according to D'Elia & DeBoer [36] as GR(% day^{-1}) = [100·Ln(W_t/W_o)]/t, where W_t is the measured biomass at day t, W_o is the initial biomass, and t is time in days. Biomass productivity (mBP, in gDW·m^{-2}·d^{-1}) was obtained as described by DeBoer and Ryther [37] as mBP = (N_t-N_o)/(t·A), where N_t is the biomass at the day t, N_o is the initial biomass, t is the time interval considered in days, and A is the superficial area of the cultivation tank.

2.5. Photosynthetic activity

Photosynthetic activity was determined through the *in vivo* chlorophyll *a* fluorescence of photosystem II (PSII) using a Diving-PAM fluorometer (Walz GmbH, Germany). Two different approaches were followed in the experiment: *in situ* measurements of effective quantum yield for the calculation of electron transport rates (ETR *in situ*) and optimal and effective quantum yield in the laboratory (*ex situ*) to calculate ETR and other fluorescence parameters from rapid light curves (RLCs) by using the artificial light provided by the Diving PAM (halogen lamp).

ETR *in situ* were obtained applying a saturating pulse to algal thalli inside the tanks, allowing the quantification of *in vivo* chlorophyll *a* fluorescence at steady state (F_t) and maximal fluorescence at light-acclimated samples (F_m'). Effective quantum yield was calculated, as Y(II) = (F_m'-F_t)/F_m'. ETR *in situ* was calculate as $ETR_{in\ situ}$ = Y(II)·PAR_m·A·F_{II}, where PAR_m is the attenuated photosynthetic active radiation in the middle tank portion (0.27 m), calculated applying attenuation coefficient (K_d) values obtained by Figueroa et al. [69] to the same species and algal densities. PAR_m was used instead of PAR in surface of the tank because the algae were moving continually from the bottom (0.54 m) to the surface of the tank due to the aeration. The parameter A

is the absorptance, which was measured at each one of the measurement's days. F_{II} (ratio of chlorophyll *a* associated to PSII) was 0.15, according to previous studies [27,70].

ETR *in situ* was quantified at different hours of local time (8:00, 9:00, 10:00, 11:00, 12:00, 13:00, 14:00, 15:00,16:00 and 20:00), and in different experimental days: 12th, 19th, 26th, 28th and 36th. Then, the integrated ETR was calculated for each tank, multiplying ETR *in situ* by the time interval, summing all daily values (calculated at each time intervals) to have an entire total of electrons·m^{-2} by treatment per day.

All calculated ETR *in situ* (for all times and days) were plotted against absorbed PAR (PAR_{abs}), to provide a real ETR per irradiance relation, for each treatment. PAR_{abs} was calculated as $PAR_{abs} = PAR_mA$. These data allowed the observation of the highest ETR produced by *G. cornea* under the four different treatments.

Rapid light curves (RLC), which represent how the fluorescence varies with increasing actinic irradiances of the Diving-PAM, were also performed in the laboratory at 9, 16, 23, 28 and 36 experimental days. Algae were incubated in darkness during 15 min in order to oxidize all the reaction centers before the beginning of the curves, and were expose during 20 s in twelve increasing irradiances (from 12 to 2900 μmol photons m^{-2} s^{-1}) by using the halogen lamp of the Diving-PAM. The parameters obtained from the RLCs and calculated from fluorescence values were: a) maximal quantum yield (F_v/F_m), b) Y(II) c) ETR and d) non-photochemical quenching (NPQ). Y(II) and ETR were calculated as explained above, replacing PAR_m by Actinic Diving-PAM incident lights. Other parameters were calculated with the following formulas: $F_v/F_m = (F_m\text{-}F_o)/F_m$ and $NPQ = (F_m\text{-}F_m')/F_m'$, where F_o is the basal fluorescence in dark, F_m is the maximal fluorescence after a saturation pulse in darkness and F_v is the variable fluorescence.

ETR and NPQ data were calculated from RLCs and were fitted according to Eilers & Peeters [71] to obtain both the maximal ETR (ETR_{max}), the slope of ETR *versus* PAR irradiance (α_{ETR}), saturated irradiance (E_k) and NPQ (NPQ_{max}). The ratio ETR_{max}/NPQ_{max} was used as indicator of the photosynthetic capacity and energy dissipation according to Figueroa et al. [27].

2.6. Bioactive compounds and bio-assays

Different bio-active compounds were extracted using freeze-dried biomass of *G. cornea* from the experimental treatments. Only mycosporine like-amino acids were determined during all the experimental period (at the beginning and 7, 13, 21, 28, and 35 days). The other variables and antioxidant capacities were determined at initial time, and after 7 and 35 culture days.

2.6.1. Total internal carbon and nitrogen content

Total carbon (TC) and nitrogen (TN) were determined from dry biomass of algae using a CNHS LECO-932 elemental analyser (Michigan, USA) in the Research Support Central Services (SCAI, University of Malaga, Spain). C and N values were expressed as mg per g of dry weight and the C:N ratio was determined.

2.6.2. Photosynthetic pigments

For chlorophyll *a* (Chl *a*) determination, 20 mg of dry weight (DW) were extracted in 1 mL of methanol 100 %. The extracts were spectrophotometrically measured at 666 and 750 nm and the Chl *a* concentrations were calculated using the equations of Wellburn [72].

For biliproteins, phycoerythrin (PE) and phycocyanin (PC) quantification, 20 mg of DW were extracted in 1 mL of phosphate buffer solution (PBS; 0.1 M, pH:6.5). The absorbances of the extracts were measured at 498, 614, 651 and 750 nm and the PE contents were calculated according to the equations of Sampath-Wiley et al. [73]. The spectrophotometer used was the UVMini-1240 (Shimadzu, Columbia, USA).

2.6.3. Total proteins

Total proteins, expressed as mg g^{-1} DW, were calculated by multiplying internal total nitrogen by the factor of 5.40 reported by Lourenço et al. [74] for a red macroalgal species (*Gracilaria domingensis*) phylogenetically close to *G. cornea*.

2.6.4. Phenolic compounds

Phenolic compounds were quantified according to Folin & Ciocalteu [75]. 20 mg of DW were extracted in 1 mL of methanol 80 %. For the reaction, 100 μL of the extract were mixed with 700 μL of H_2Od, 50 μL of Folin-Ciocalteau phenol reactive (Sigma-Aldrich, USA) and 150 μL of $NaCO_3$ 20 %. After vortexing and incubation (2 h, in darkness and at 4 °C), absorbances of extracts reactions were measured at 760 nm. Phloroglucinol was used as standard.

2.6.5. Mycosporine-like amino acids (MAAs)

MAAs were determined by HPLC (Waters 600, Barcelona, Spain) as described Korbee-Peinado et al. [47]. 20 mg of DW algal biomass were extracted in methanol 20 % at 45 °C in a thermo-bath during 2 h. After centrifuged, the supernatant (700 μL) was dried in a vacuum centrifuge, redissolved in 700 μL of methanol and filtered through a 0.2 μm filter. MAAs were analyzed using a sphereclone C8 column (Phenomenex, Germany), an isocratic flow of 0.5 mL min^{-1} and a mobile phase of 1.5 % methanol and 0.15 % acetic acid in ultrapure water. The detection was made using a photodiode array (PDA) detector. Secondary standards were used for the identification of MAAs and the quantification was performed using published molar extinction coefficients (ε) of the different MAAs [76].

2.6.6. Antioxidant capacity – ABTS

The ABTS assay was performed as described Re et al. [77]. The $ABTS^{+\bullet}$ was generated by a reaction of 7 mM ABTS and 2.45 mM potassium persulfate in phosphate buffer solution (PBS: 0.1 M; pH:6.5), this reaction was stored in dark for 12-16 h at room temperature to ensure the complete formation of the radical. For this assay, the same extracts prepared for phycoerythrin quantification were used. 50 μL of the extract was mixed with 940 μL of PBS and 10 μL of $ABTS^+$ solution. After 8 min of incubation, absorbance was measured at 413 nm. Trolox was used as standard, as being an analogue molecule to Vitamin E (6-hydroxy-2,5,7,8-tetramethylchroman-2-carboxylic acid). Results were expressed as μmol Trolox equivalent μmol (TE) g^{-1} DW.

2.7. Statistical analysis

Data were analyzed with different statistical tools (software STATISTICA V.7 and Primer 6). Firstly, as the time of obtaining data was different for each variable, regression linear analyses of the dependent variable responses against the time were conducted. It was done to growth rates, productivity, %NUE, NUR, ETR *in situ vs.* absorbed PAR, MAAs and MAA productivity. With these fittings, intercepts, slopes, and *p*-values were determined, allowing the understanding of how the data changed over the time.

Parametric values were submitted to the previous assumptions of normality and homogeneity of variances tests, with Shapiro-Wilks and Cochran tests, respectively. After, the influence of radiation and nutrients availability were assessed by a bifactorial analysis of variance (ANOVA). The factor levels were outdoor and greenhouse condition, for radiation factor, and high nitrogen (HN) or low nitrogen (LN) availability, for nutrient factor. Significance level was fitted to $\alpha = 0.05$. Significant influences were observed when $p\text{-value} < 0.05$. In such cases, the means were compared with *a posteriori* test of Student-Newman Keuls. The following dependent variables were evaluated with this procedure: slopes of growth rates, biomass productivity, %NUE, NUR, ETR *in situ*, MAAs and MAA productivity; and also the data were compared with a fixed period of time to the variables: growth rates, biomass productivity, %NUE, NUR, integrated ETR, F_v/F_m, $ETR_{max}/$

NPQ_{max}, total MAAs, MAA productivity, chlorophyll *a*, phycoerythrin, phycocyanin, total of proteins, polyphenols, antioxidant capacity assessed by ABTS, total C, N, and C:N ratio. In addition, initial measurements were compared with the other treatment conditions with a t-student test ($p < 0.05$). With the data obtained at the 7th and 35th experimental days, all dependent variables were compared with a correlation analysis of Pearson.

A principal component analysis (PCA) was done with the dependent variable data considering the treatment combinations of nutrient and radiation availability. Previously, data were log(x + 1) transformed. Later, their correlations with the two PCA axes were assessed with a Pearson correlation test. These analyses were conducted with the software Primer 6.

3. Results

Irradiance and daily integrated irradiance in the experimental facility are presented in Fig. 2A and B, and Table S1. Fig. 2A shows daily average irradiance that was reached in the water surface of the outdoor and under greenhouse tanks. Clearly, the greenhouse structure was able to sharply reduce UV radiation. Outdoor samples received a total accumulated UV-A daily integrated irradiance 28 times higher than those in tanks under greenhouse during the entire experimental period (Table S1). Maximal outdoor PAR reached 600 μmol photons m^{-2} s^{-1}, while inside the greenhouse, the higher value was around 420 μmol photons m^{-2} s^{-1} (Fig. 2A, Table S1). Therefore, daily PAR integrated irradiances inside the greenhouse were lower than those measured outdoor (Fig. 2B, Table S1). Values varied from 19 to 36 mol photons m^{-2} inside the greenhouse and 27.7 to 52.5 mol photons m^{-2} in outdoor conditions. Maximal value of UV-A radiation inside the greenhouse was 0.2 W m^{-2} and outdoor was 9.5 W m^{-2}. Temperature variations were similar in both treatments (G and O) (Fig. 2C). Greenhouse tanks showed average temperature between 22.3 and 24.2 °C, with minimal and maximal values of 21 °C and 27.2 °C, respectively. In the outdoor tanks, mean temperatures varied from 22.1 °C to 24.8 °C (Fig. 2C, Table S1) and maximal temperatures in the last days of the culture period reached 30 °C.

Nitrogen uptake efficiencies (%NUE) and nitrogen uptake rates (NUR) during the experimental period are presented in Fig. 3. N-uptake (efficiency and rates) varied differently during the time according to the treatments (Table S2), with significant regression slopes of %NUE observed to O-LN, G-HN and O-HN, while samples NUR did not showed variations over the time, as none of the slopes were significant ($p > 0.05$, Table S2). In the case of %NUE, slopes of all treatments were negatives, indicating that NUE decreased over the time (Fig. 3, Table S2). However, they were not differently affected by the treatments of radiation, nutrient availability or the interaction between nutrient and radiation (Table S3). When the efficiency was evaluated at each time separately, it was possible to detect a clear influence of the interaction between radiation and nutrient availability at the 8th and 28th experimental days. In the other periods, only nutrient availability caused significant variability to the NUE (Table S4). Data of %NUE were higher at G-LN and O-LN, with values higher than 80 % of efficiency at the 8th, 15th, 23rd and in the last 35th days. An acute reduction to values around 40 % to O-LN and 60 % to G-LN were observed in the 28th experimental day (Fig. 3A). In the case of NUR, significant effects of the interaction between nutrient and radiation were observed at 8th day, while the factor nutrient availability was responsible for causing significant differences to the data at days 28th and 35th (Table S4). Algae in tanks treated with O-HN showed the highest NUR values at the starting period, with rates values higher than 25 mmol m^{-2} h^{-1}. Along the experimental period, samples receiving HN showed higher NUR also at the last two measurements, in days 28th and 35th. In this last period, values of NUR were higher than 30 mmol m^{-2} h^{-1} under HN (Fig. 3B).

The differences in N-uptake according to the treatments were not reflected in prominent differences of growth rates or biomass production by *G. cornea* (Fig. 4). Linear regression analyses showed significant negative slopes for samples under treatments outdoor, indicating reduction of growth rates capacity over the time (Table S2). In addition, when slopes obtained from different treatments were compared, they also were statistically similar, without effects of nutrient or radiation in variations of growth rates of biomass productivity (Table S3). The growth rates and biomass productivity at each experimental sampling day (7, 13, 20, 28, and 35 days) were also similar under the four experimental conditions (Fig. 4, Table S4).

Daily photosynthetic responses of *G. cornea* are presented in Figs. 5 and 6. ETR increased in all treatments from the morning to the noon and then decreased from noon to the end of the day. The highest values of daily ETR were recorded in O-HN treatment (13:00 h at day 12th), remaining high in the following hours, and decreasing to values around 40 μmol electrons m^{-2} s^{-1} at the end of the day. High ETR values were reached at day 12th under O-LN and G-HN treatments (at 15:00 and 16:00, respectively, Fig. 5A). At day 19th, high values of ETR were reached under O-HN and O-LN at 14:00 and 16:00, respectively (again higher than 90 μmol electrons m^{-2} s^{-1}), while the other treatments presented peaks with lower ETR *in situ* values (Fig. 5B). The highest PAR daily integrated irradiance at outdoor was 49.8 mol photons m^{-2} at day 26th. However, observed ETR *in situ* values were not so high as the obtained during the two previous days of measurements (Fig. 5C). At day 28th, peaks of ETR *in situ* were again higher than 80 μmol electrons m^{-2} s^{-1} in all treatments, being recorded at different times for each treatment: the highest ETR *in situ* was found at 16:00 under LN, while in HN, these values were found earlier, at 14:00 (Fig. 5D). In the last measurements at day 36th, peaks of ETR *in situ* presented similar characteristics as at day 26th, with higher values observed under outdoor conditions (Fig. 5C and E).

The integrated ETR of *G. cornea* calculated from the data in Fig. 5 are presented in Fig. 6. The values of this integrated parameter varied from 0.7 ± 0.04 in G-LN at day 36th, to 1.4 ± 0.13 mol electrons m^{-2} s^{-1} in O-HN, at day 12th (Fig. 6). An evident pattern of higher integrated ETR was observed at outdoor conditions compared to those under greenhouse, regardless of time. Radiation was the fundamental factor for causing variations of integrated ETR in all measured days (Table S4), but in the last one (36th), effects were also caused by the nutritional availability. The highest integrated ETR were recorded at day 12th in O-HN and O-LN conditions. Values of this parameter in algae from outdoor were always higher than those inside of the greenhouse (Fig. 6). As a general pattern, increases in the PAR irradiance increased values of ETR of *G. cornea*. Slopes of ETR *vs.* absorbed PAR are represented in the Fig. S1, and they were significantly positive (Table S2). The slope values found in LN treatments were significantly higher than those found in HN treatments (effects caused by the N and P-availability, Table S3). However, the highest ETR values observed for *G. cornea* were found at O-HN, followed by O-LN. It must be mentioned that this species was able to absorb >1000 μmol photons m^{-2} s^{-1} and allowed the transport of >80 μmol electrons m^{-2} s^{-1} (Fig. S1).

Photosynthetic parameters derived from RLC measurements taken in the laboratory (indoor) are presented in Fig. 7. The maximum quantum yield, F_v/F_m, was initially 0.64 ± 0.03, and remained similar only in algae cultivated in G-LN after 9 days. All other F_v/F_m values were lower than the initial one (*t*-test, $p < 0.05$). In general, few oscillations were found in this parameter (Fig. 7A). N-availability and radiation as isolated factors significantly affected the variation of F_v/F_m in the 9th and 16th days. In the following week (23rd day), only N-availability influenced significantly F_v/F_m responses (Table S4). A reduction of F_v/F_m of HN samples in comparison to LN treatment was observed till the 23rd day. However, it is remarkable that since day 28th, all values of this parameter were similar in all treatments till the end of the experiment (day 36th), indicating that *G. cornea* kept its photosynthetic potential, and any possible inhibition at day 16th was recovered (Fig. 7A). ETR_{max}/NPQ_{max} ratios increased substantially in all experimental measurements in comparison to the initial value (Fig. 7B). ETR_{max}/NPQ_{max} variations

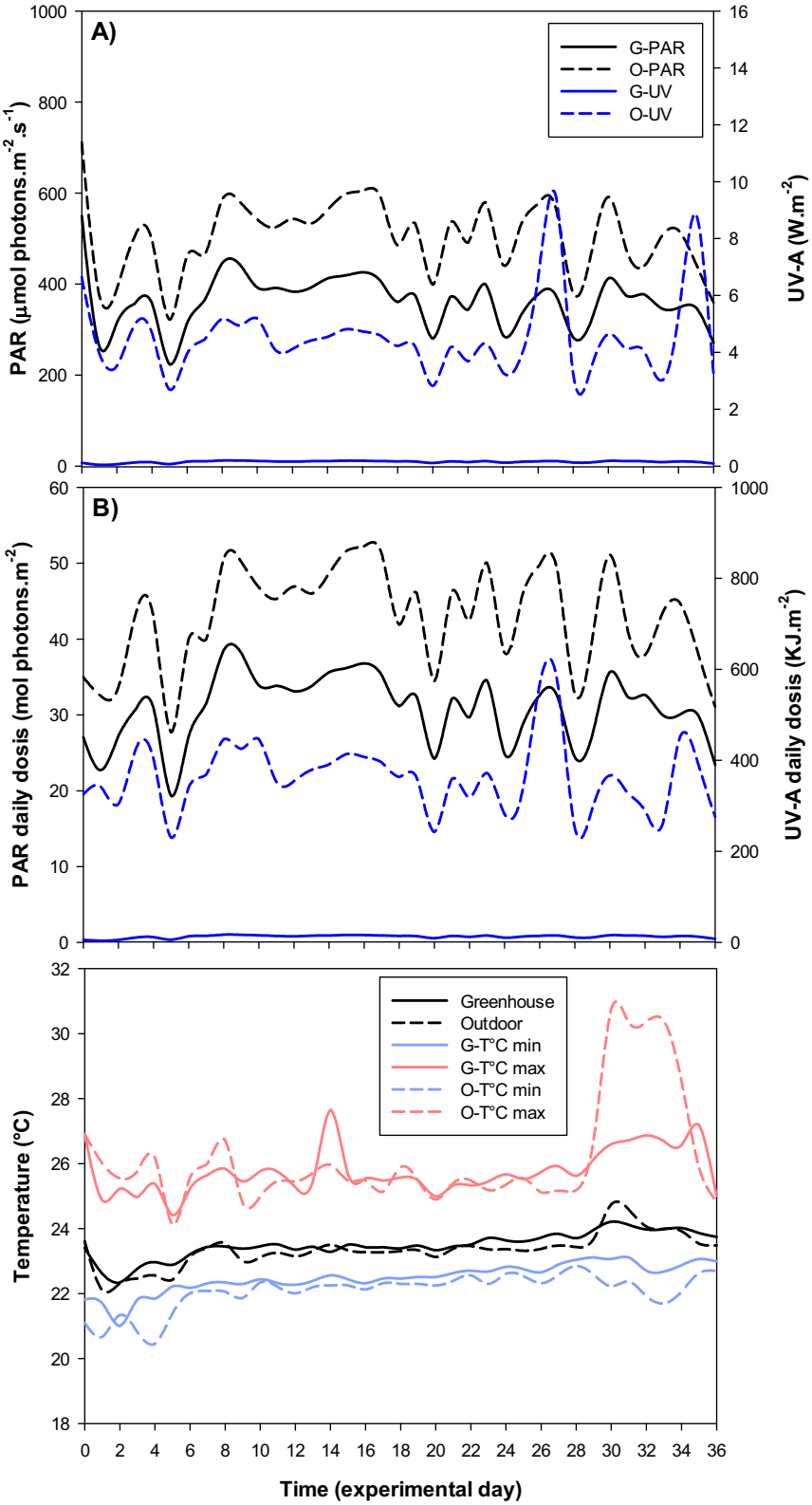

Fig. 2. Solar radiation during experimental period in the open system setup at Spanish Bank of Algae, Taliarte. (A) Data were measured as irradiance considering photosynthetic active radiation (PAR, λ = 400-700 nm) and UV-A radiation (UVA, λ = 320-400 nm). (B) Daily integrated irradiance of PAR and UV-A. (C) Maximal, minimal and average temperatures in the air in outdoor place (O) and in the greenhouse (G) throughout the experimental period of 35 days (see Fig. 1).

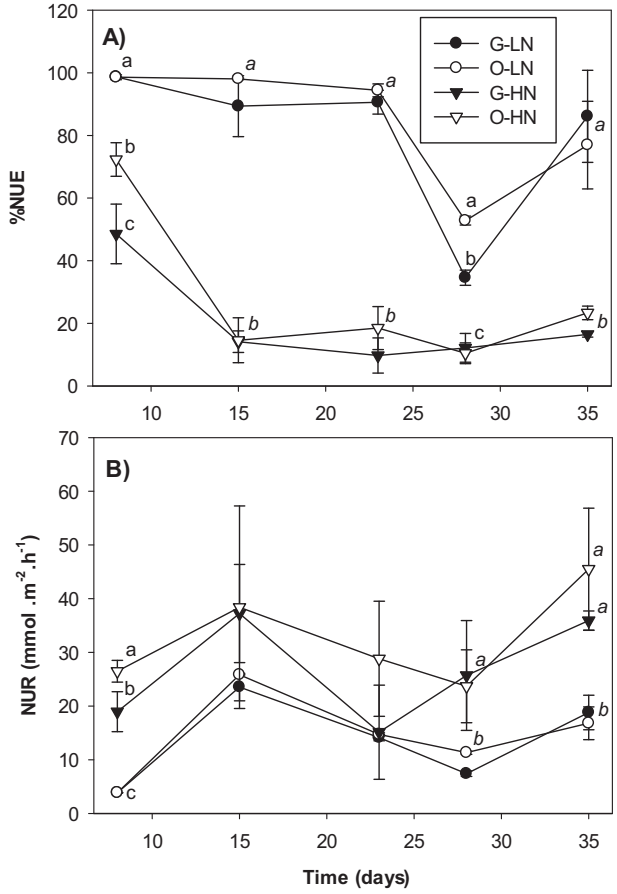

Fig. 3. Nitrogen uptake efficiency (NUE %) (A) and nitrogen uptake rates NUR (mmol m^{-2} h^{-1}) (B) by *G. cornea* at 8, 15, 23, 28 and 35 days under the different experimental conditions: outdoor under high nutrient (O-HN) or low nutrient (O-LN) supply and indoor (greenhouse) under high nutrient (G-HN) and low nutrient (G-LN) supply. Each value is represented as mean ± S.D. (error bars, $n = 3$). Comparisons among data were done at each time period separately. Significant variations are represented by different letters when significant differences caused by interaction between N-availability and radiation were found. Italic letters represent the effect of the isolated factor nutrient availability.

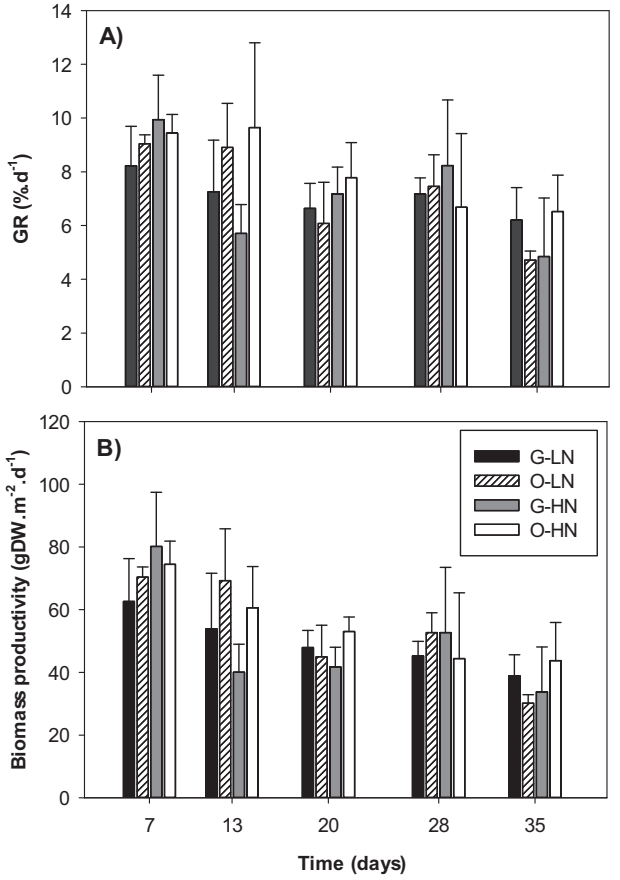

Fig. 4. Biomass variability evaluated as: (A) Growth rates (%·d^{-1}) and (B) productivity (g DW m^{-2} d^{-1}) of *G. cornea* at 7, 13, 20, 28 and 35 days cultivated under different experimental condition: outdoor under high nutrient (O-HN) or low nutrient (O-LN) supply and indoor (greenhouse) under high nutrient (G-HN) and low nutrient (G-LN) supply. Each value is represented as mean ± S.D. (error bars, $n = 3$).

were influenced by N-availability (Table S4) in all measured experimental days. Consequently, data of this ratio were higher to samples grown with HN in comparison to those which received LN (Fig. 7B).

The pigmentation and morphology of thalli changed through the time and were affected by the treatments as showed in Fig. 8 and Table 1 at days 7^{th} and 35^{th} of culture. After 7 days, thalli presented similar brownish to reddish coloration, without marked visual differences. However, at the end of the experiment (day 35), thalli grown in O-LN were yellowish, and those in G-HN were darkened. Samples in G-LN and O-HN showed coloration closed to that of samples at day 7^{th}. O-HN treated thalli were visually more branched than the others (Fig. 8). Photosynthetic pigment concentrations presented different response patterns (Table 1). While chlorophyll *a* (Chl *a*) was influenced by the interaction between radiation and nutrient at day 7^{th}, in the case of accessory phycoerythrin, only nutrient availability was relevant to cause significant variations (Table S5). Chl *a* showed some variations throughout the time under the different treatments with respect to the initial time. Chl *a* decreased in LN and O-HN at day 7^{th} (values reduced to half, from 0.2 to 0.1 mg gDW^{-1}), and in O-LN at day 35^{th} in comparison to the initial amounts (Table 1), recovering quantities similar to those at the beginning of the experiment under HN and G-LN. In the case of phycobiliproteins, PC and PE were different only in HN after 35 days in comparison to the initial thalli. In the case of PC, no effects were detected by the treatments at each separated experimental day. PE contents were 2.5 times higher in samples cultivated with HN when compared to those at LN, after 7 days and remained 2.3 times higher after 35 days. (Table 1).

Biochemical composition of *G. cornea* varied during the experimental period and according to the treatments. Total proteins increased in HN at day 7 and in all treatments after 35 days of culture in comparison to the initial time (Table 1). While in the 7^{th} day the effect was related to nutrient availability, in the 35^{th} day, the interaction between radiation and nutrient was responsible for causing differences in the protein contents (Table S5). After 7 days, samples cultivated with HN showed two times higher protein contents than those under LN. A similar response was detected after 35 days, but in that occasion, samples in greenhouse showed the maximal quantity of total proteins detected in the entire experiment (283.2 ± 20.73 mg g^{-1} DW), even higher amounts than those in outdoor conditions (Table 1). Phenolic compounds increased during the experiment in comparison to the initial amount (t-test, $p < 0.05$). Separated effects of radiation and nutrient availability were observed at day 7 (Table S5). Samples in the greenhouse showed lower phenolic compounds quantity than those outside, and those with HN presented a higher amount of phenolics than those under LN (Table 1). At day 35^{th}, polyphenols concentration values were statistically similar in all treatments, with an average of 49.5 ± 9.45 mg g^{-1} DW (Table 1).

Elemental and bioactive composition of *G. cornea* is presented in

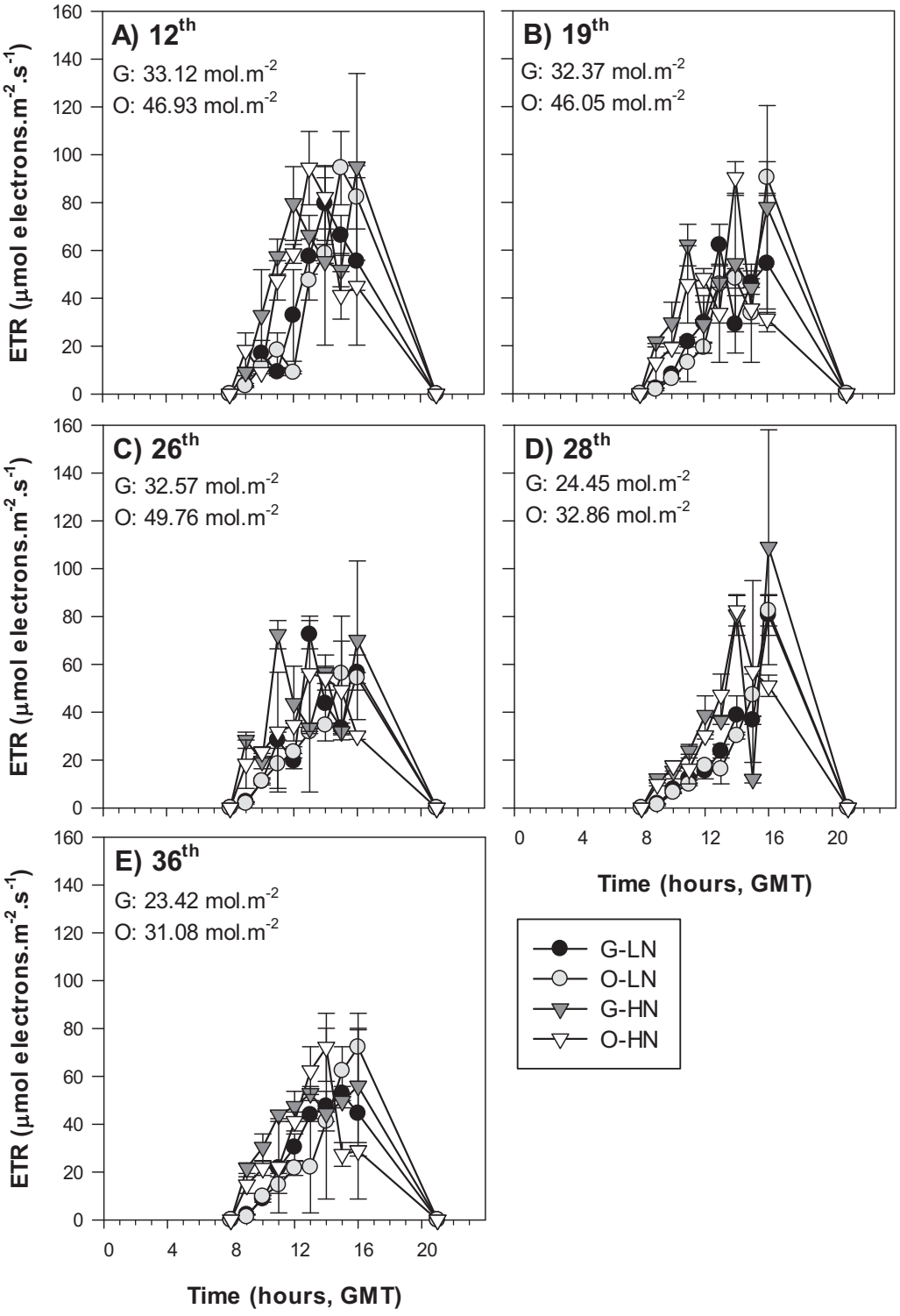

Fig. 5. Daily measurements of *in situ* electron transport rate (ETR *in situ*) expressed in µmol electrons m^{-2} s^{-1} of *G. cornea* at 12, 19, 26, 28 and 36 days cultivated under different experimental conditions: outdoor under high nutrient (O-HN) or low nutrient (O-LN) supply and indoor (greenhouse) under high nutrient (G-HN) and low nutrient (G-LN) supply. Each value is represented as mean ± S.D. (error bars, $n = 3$). The daily integrated irradiances of PAR expressed as mmol photons m^{-2} in outdoor (O) and in the greenhouse (G) are indicated in the upper part of each figure.

Table 1. No significant variations were found for C content, which remained around the average of 220.8 ± 13.98 mg gDW^{-1}. N internal content followed the same pattern of response above described for total internal proteins, considering that one was directly related to the other. In the case of the differences of C:N ratios (Table 1), they were caused by the nutrient availability after 7 days and the interaction of this factor with radiation after 35 days (Table S5). Initial C:N ratio remained similar in the samples of LN after 7 days (t-student, $p > 0.05$), and decreased to values lower than 10 in algae which received HN. In the last experimental day, the C:N ratio was very low in comparison to initial ratio ($p < 0.05$, t-student test). G-LN samples presented the ratio close to 12, while those samples at G-HN and O-HN showed C:N ratio of 4.6 and 6, respectively (Table 1).

Total mycosporine-like amino acids (MAAs) and their productivity are showed in Fig. 9. Both showed significant and positive linear regression in all treatments performed with the biomass against the time periods (Table S2), indicating that MAAs increase over the time. While the slopes of total MAAs were similar among each other, MAA

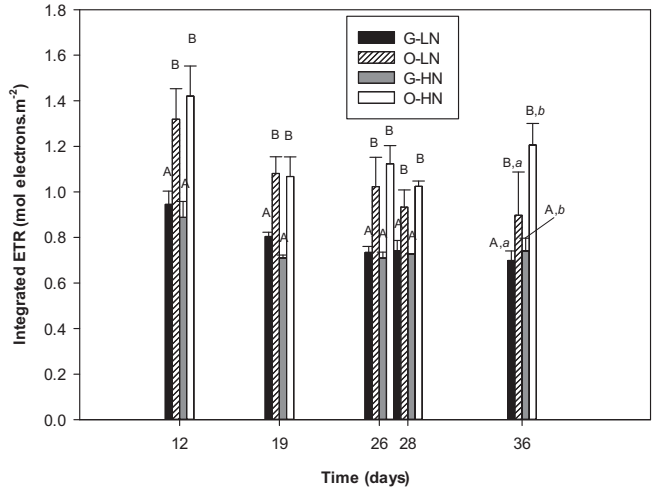

Fig. 6. Daily integrated electron transport rate (integrated ETR) expressed in mol electrons m^{-2} of *G. cornea* at 12, 19, 26, 28 and 36 days cultivated under different experimental conditions: outdoor under high nutrient (O-HN) or low nutrient (O-LN) supply and indoor (greenhouse) under high nutrient (G-HN) and low nutrient (G-LN) supply. Each value is represented as mean ± S.D. (error bars, $n = 3$). Comparisons among data were done at each time period separately. Different italic letters represent the differences caused by the isolated factor nutrient availability. Different capital letters are representing the differences caused by the isolated factor radiation.

productivity was significantly affected by the interaction of radiation and N-availability (Table S3). In the case of total MAAs, the slopes ranged from 0.08 ± 0.01 to 0.12 ± 0.02 (Table S2). However, the productivity of MAAs resulted to be faster and higher over the time for O-HN in comparison to the other three treatments, achieving the slope of 4.5 ± 0.22 (Table S2). The radiation available was fundamental for determining significant differences in MAA content in all experimental days evaluated. In addition, the factor of nutrient availability showed influence in the total of MAAs on 13th, 20th and 28th experimental days. At day 7th, MAA content was twice increased under outdoor conditions than that for algae grown under greenhouse, and this situation was kept till the end of experimental period. At the 20th and 28th days, the HN treated samples presented higher amounts of MAAs than those with LN (Fig. 9A). O-HN treatment caused a prominent increase of MAAs in comparison to the other conditions at days 13th, 20th and 28th. Thalli cultivated outdoor reached total values of 5.1 ± 0.47 and 4.8 ± 0.78 mg of MAAs per g DW, when supplied with HN or LN, respectively, after 35 days (Fig. 9A).

In the case of algal MAAs productivity, radiation was significant to causing significant differences after 7 days, while in all other experimental periods, that variations were caused by the interaction between N-availability and radiation (Table S4). It is noticeable that the algae in O-HN presented a productivity higher than 100 mg MAAs m^{-2} d^{-1} already at day 7th and remained as the best condition for MAA production in the entire experimental period, reaching the productivity of >200 mg of MAAs by m^2 per day (Fig. 9B).

Five different MAAs were identified in *G. cornea* by HPLC: palythine, asterina-330, shinorine, porphyra-334 and palythinol. These types were always present in the *G. cornea* thalli in any of the cultivation conditions (Fig. 10). Asterina-330 was the dominant MAA in the initial time and after 7 days of culture except under O-LN, being palythinol the dominant MAA. An increment of the palythinol percentage was observed along the time, with respect to the other MAA-types, with reducing palythine and asterina-330. These differences were evident when comparing the different times (initial, after days 7 and 35, Fig. 10). After 35 days, values for asterina-330 were higher under HN compared to LN treatments (Fig. 10).

Antioxidant capacity measured using ABTS assay in *G. cornea*

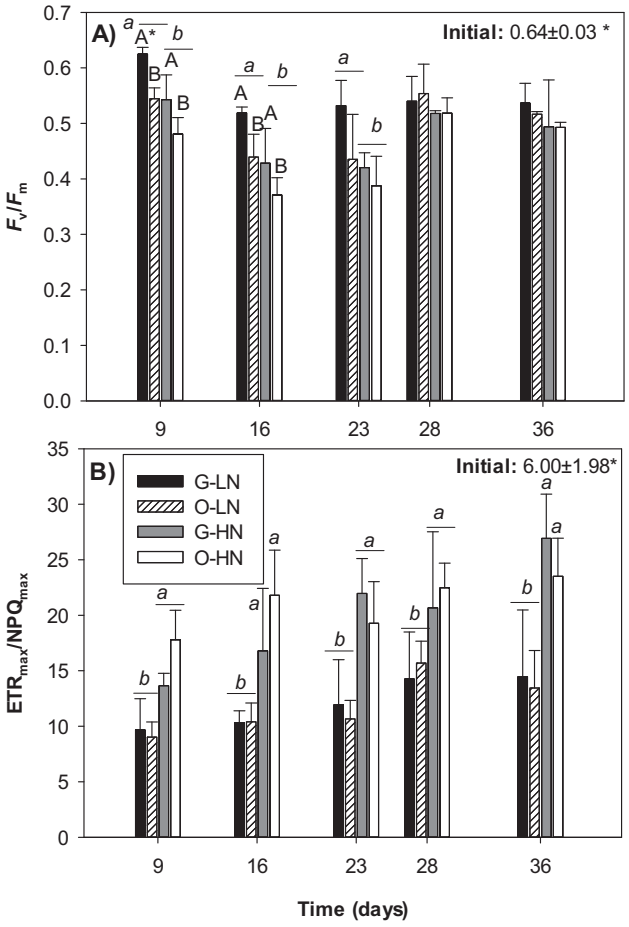

Fig. 7. *In vivo* chlorophyll *a* fluorescence parameters as maximum quantum yield (F_v/F_m) (A) and ETR_{max}/NPQ_{max} ratio (B) obtained from rapid light curves produced under laboratory conditions (*ex situ*) of *G. cornea* at 9, 16, 23, 28 and 36 days cultivated under different experimental conditions: outdoor under high nutrient (O-HN) or low nutrient (O-LN) supply and indoor (greenhouse) under high nutrient (G-HN) and low nutrient (G-LN) supply. F_v/F_m and ETR_{max}/NPQ_{max} ratio at initial time are indicated in the figures. Each value is represented as mean ± S.D. (error bars, $n = 3$). Comparisons among data were done at each time period separately. Different italic letters represent the differences caused by the isolated factor nutrient availability. Different capital letters are representing the differences caused by the isolated factor radiation. Initial data and all treatment conditions were compared in pairs by using a t-student test, and when the comparison showed no significant differences ($p > 0.05$), an asterisk was included to indicate which of the bars could be considered equal to initial values.

extracts significantly increased during the experiment, in comparison to the initial value (Table 1, *t*-test, $p < 0.05$). The increment was at least 4 times in all treatments, from 10.40 ± 0.96 to >40 μmol TE g^{-1} DW. After 7 days, separated effects of radiation and nutrients were found (Table S5). The extracts of samples cultivated in the greenhouse showed higher antioxidant capacity than those in outdoor, and those with LN showed also higher antioxidant capacity than those at HN. At day 35, no differences among treatments were found (Table 1, Table S5).

Correlations between different physiological responses of *G. cornea* are presented in the Table S6. Some of them must be highlighted, for example the positive correlation between integrated ETR and growth rates or biomass productivity ($r = 0.456$ and $r = 0.464$, respectively; $p < 0.05$). ETR_{max}/NPQ_{max} ratio (relation between photosynthetic capacity and energy dissipation) was related to NUR, photosynthetic pigments (Chl *a* and phycobiliproteins) and MAAs. Integrated ETR was not related to the accumulation of bio-active compounds (except negative correlation to Chl *a*), whereas growth and biomass productivity were negatively

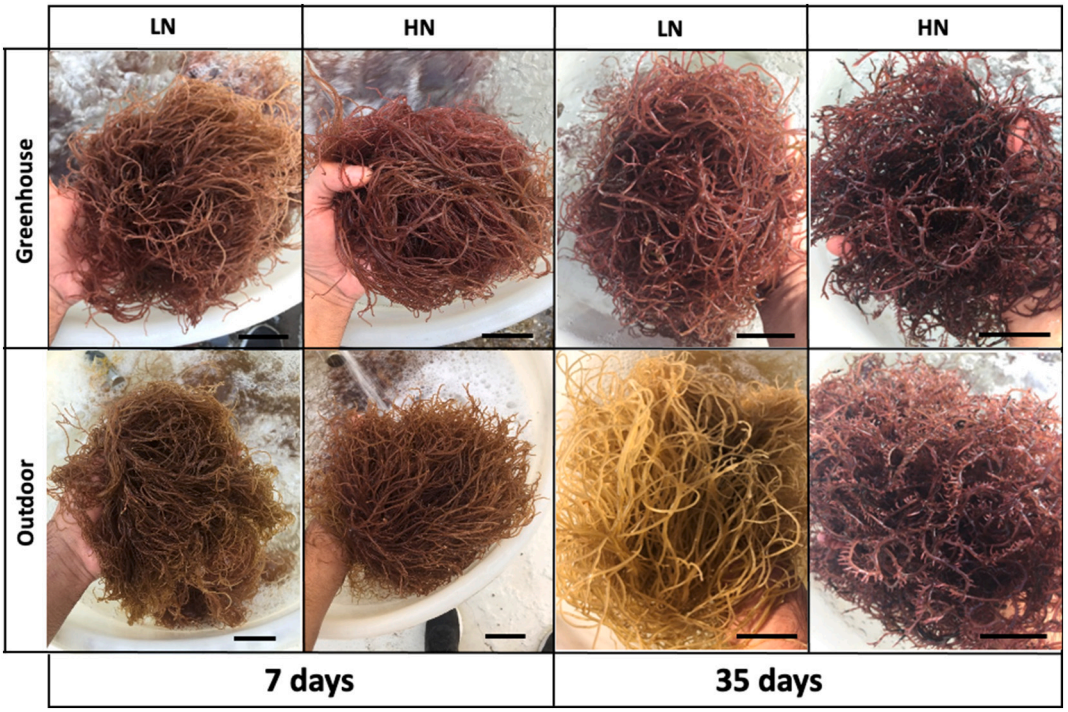

Fig. 8. Morphology and thalli colors of *G. cornea* at 7 and 35 days of culture in the different experimental conditions: outdoor, receiving full solar radiation, under high nutrient (HN) or low nutrient (LN) supply, and indoor (greenhouse) under high nutrient (HN) and low nutrient (LN) supply. Bar scale size is equal to 5 cm.

correlated to the pigments content (Chl *a* and phycobiliproteins). In general, nitrogen-containing compounds were positively correlated among each other (Table S6). The capacity of biofiltration (NUR) and efficiency of biofiltration (%NUE) were not correlated to growth or the biomass productivity. However, NUR was positively correlated to pigments (Chl *a* and biliproteins), proteins and UV photoprotectors-antioxidants (MAAs and polyphenols) and total internal C and N. On the other hand, the correlation pattern of the efficiency of biofiltration (%NUE) was the reverse, *i.e.*, negative correlation to pigments and MAAs. Antioxidant capacity determined by ABTS was negatively correlated to growth and biomass productivity.

Principal component analysis (PCA) of dependent variables measured in *G. cornea* cultivated under outdoor and greenhouse conditions with nutrient additions is presented in the Fig. 11. The PC1 axis was responsible for 72.9 % of the data variation, while the second PC2 axis caused 11.7 % of biological responses of *G. cornea* cultivated in tanks. The ETR_{max}/NPQ_{max} ratio, NUR, photosynthetic pigments, MAAs, and total proteins were strongly negatively correlated with PC1, while % NUE and photoprotective compounds (MAAs and polyphenols) were positively correlated with PC2. Photoprotective compounds (phenolics and MAAs) were grouped together, in an opposite position in comparison to the growth and integrated ETR. Moreover, the PCA indicates that the treatments containing HN were those responsible for regulating the variability of photosynthetic pigments, total proteins, NUR, ETR_{max}/NPQ_{max} ratio and also growth rates and integrated ETR responses (Fig. 11).

4. Discussion

Macroalgae have been successfully used as biofilters of fishpond effluents (IMTA systems) or other waste waters [7,10] and the produced biomass can be used for the production of high added value biocompounds such as proteins, photoprotectors or antioxidants, among others [60,78]. However, most of the studies have been conducted during short-term periods (less than two weeks) [63,79–82]. To demonstrate the real use of IMTA systems in land facilities to produce algal high value biocompounds, it is necessary to increase the time of the experiments. In this study, algae cultured during 35 days have demonstrated high ammonium biofiltration capacity and the accumulation of high value biocompounds.

In relation to the biofiltration capacity, a high NUR (30-50 mmol m^{-2} h^{-1}) under O-HN treatment was observed in this study. High biofiltration capacity of Gracilariales has been already reported [61,83,84]. The species used in this work, *G. cornea,* was an efficient biofilter of inorganic nitrogen (NH_4^+), reaching NUE values close to 99 %. NUR values obtained in this study were higher than those observed in green algae of the family Ulvaceae, as *Ulva rotundata* (1.45 g N m^{-2} d^{-1}) reported by Mata & Santos [83], and other red and brown algae [64]. Additionally, *G. cornea* reached similar biofiltration capacities as other high algal biofilters as the red alga *Asparagopsis armata* [84]. The expression of NUR in terms of tank area was suggested by Jiménez del Río et al. [67], since algae are growing at high algal density in tanks and the main light exposure and consequently photosynthetic activity and nutrient uptake is related to the surface exposure of the tank [60,69]. In addition to N-biofiltration, high assimilation of phosphate has been also reported in IMTA systems by using *Ulva* and *Gracilaria* species [85,86].

The nutrient assimilation is expected to be related to photosynthetic capacity. Photosynthesis is dependent on light quality and quantity, and nutrient availability. Photosynthetic capacity as integrated ETR (*in situ* measurements) reached the highest values under high nitrogen availability (as photosynthetic substrate) and full solar radiation (O-HN) but with similar values than that obtained under O-LN. Thus, light conditions seem to have dominant effects on photosynthetic capacity. However, when ETR is determined in the laboratory as RLCs (*indoor*), the ratio between maximal photosynthetic capacity and maximal energy dissipation (ETR_{max}/NPQ_{max}) were higher under HN treatment both, under greenhouse (G) and outdoor (O), showing a high effect of N availability on photosynthetic capacity in relation to photoprotective strategies. In addition, integrated ETR was correlated to growth and biomass productivity, but not to N-biofiltration (NUE or NUR). In contrast, ETR_{max}/NPQ_{max} was not related to growth and biomass productivity, but it presented a positive correlation to NUR and the

Table 1
Bioactive and elemental compounds and antioxidant capacity by ABTS method obtained in *G. cornea* at the beginning, and after 7 and 35 days of cultivation under different experimental conditions: outdoor under high nutrient (O-HN) or low nutrient (O-LN) supply and indoor (greenhouse) under high nutrient (G-HN) and low nutrient (G-LN) supply. The following compounds were evaluated: Chlorophyll *a* (Chl *a*), phycoerythrin (PE), phycocyanin (PC), total proteins, polyphenols, total internal C and N, and C:N ratio. Each value is represented as mean ± S.D. ($n = 3$). Comparisons among data were done at each time period separately. Different letters represent the differences caused by the interaction between nutrient availability and radiation. Different italic letters represent the differences caused by the isolated factor nutrient availability. Different capital letters are representing the differences caused by the isolated factor radiation. Initial data and all treatment conditions were compared in pairs by using a t-student test, and when the comparison showed no significant differences ($p > 0.05$), an asterisk was included to indicate which of the bars could be considered equal to initial values.

		Chl-*a* (mg gDW^{-1})				PE (mg gDW^{-1})				PC (mg gDW^{-1})				TotalProteins (mg gDW^{-1})				Polyphenols (mg gDW^{-1})				ABTS (μmolTEgDW^{-1})				C (mg gDW^{-1})				N (mg gDW^{-1})				C : N			
Initial		0.21	±	0.01	*	0.48	±	0.28	*	0.22	±	0.11	*	57.94	±	4.90	*	13.53	±	1.48		10.40	±	0.96		222.97	±	20.80	*	10.73	±	0.91	*	20.91	±	3.04	*
7 days	G-LN	0.10	±	0.02	a	0.18	±	0.20	*	0.27	±	0.25	*	49.09	±	7.53	a*	22.01	±	4.96	a	62.02	±	6.11	A,*a*	214.73	±	23.97	*	9.09	±	1.39	a*	23.75	±	1.38	a*
	O-LN	0.08	±	0.05	a	0.14	±	0.16	*	0.20	±	0.11	*	47.07	±	12.91	a*	25.88	±	4.49	a	53.60	±	2.17	B,*a*	213.43	±	4.35	*	8.72	±	2.39	a*	25.85	±	7.50	a*
	G-HN	0.22	±	0.02	b*	0.35	±	0.13	*	0.27	±	0.06	*	119.29	±	10.67	b	26.79	±	2.36	a	49.12	±	4.36	A,*b*	197.83	±	9.98	*	22.09	±	1.98	b	8.98	±	0.46	b
	O-HN	0.09	±	0.03	a	0.44	±	0.19	*	0.36	±	0.19	*	112.07	±	8.39	b	34.81	±	0.82	b	42.40	±	6.73	B,*b*	211.50	±	10.67	*	20.75	±	1.55	b	10.22	±	0.85	b
35 days	G-LN	0.22	±	0.07	*	0.78	±	0.58	*	0.52	±	0.33	*	102.76	±	28.40	a	50.62	±	5.61		53.43	±	14.88		218.20	±	17.82	*	19.03	±	5.26	a	11.92	±	2.44	c
	O-LN	0.11	±	0.04		0.47	±	0.34	*	0.33	±	0.08	*	139.10	±	19.97	a	55.54	±	17.88		65.24	±	11.01		226.40	±	16.78	*	25.76	±	3.70	a	8.87	±	0.96	b
	G-HN	0.26	±	0.05	*	1.63	±	0.42		0.72	±	0.18		283.24	±	20.73	c	35.75	±	6.57		54.30	±	6.36		242.17	±	9.38	*	52.45	±	3.84	c	4.64	±	0.46	a
	O-HN	0.23	±	0.08	*	1.32	±	0.52		0.68	±	0.24		212.94	±	4.12	b	55.90	±	26.51		56.59	±	6.16		239.77	±	7.28	*	39.43	±	0.76	b	6.08	±	0.26	a

Fig. 9. Mycosporine-like amino acids (MAAs) obtained in *G. cornea* at 7, 13, 20, 28 and 35 days cultivated under different experimental conditions: outdoor under high nutrient (O-HN) or low nutrient (O-LN) supply and indoor (greenhouse) under high nutrient (G-HN) and low nutrient (G-LN) supply. (A) Total MAA content, expressed as mg g^{-1} DW, and (B) MAA productivity expressed as mg m^{-2} d^{-1}. Each value is represented as mean ± S.D. (error bars, $n = 3$). Comparisons among data were done at each time period separately. Different letters represent the differences caused by the interaction between nutrient availability and radiation. Different italic letters represent the differences caused by the isolated factor nutrient availability. Different capital letters are representing the differences caused by the isolated factor radiation. Initial data and all treatment conditions were compared in pairs by using a t-student test, and when the comparison showed no significant differences ($p > 0.05$), an asterisk was included to indicate which of the bars could be considered equal to initial values.

accumulation of some biocompounds. The ratio ETR_{max}/NPQ_{max} is suggested as a good indicator of the ratio of production related to energy loss [95]. This expression was proposed as the first time by Figueroa et al. [87]. They showed that UV-B exposure decreased the ETR_{max}/NPQ_{max} ratio as consequence of increased photoinhibition. The highest value of this ratio indicates better physiological state and more relative energy available for growth and/or the accumulation of bio-active compound. In the first weeks of culture, a slight photoinhibition was observed according to the decrease of F_v/F_m parameter. Significant differences were observed between LN and HN treatments. However, in the last two periods of measurement, no differences among the treatments were observed, indicating acclimation to culture conditions.

ETR values determined *in situ* under solar radiation were higher than those obtained in the RLCs (*ex situ*) by using artificial light (halogen lamp provided by the Diving PAM). Maximal ETR *in situ* at noon time reached values of 100–150 μmol electrons m^{-2} s^{-1}, whereas ETR_{max} values in the laboratory (RLCs) were around 10–14 μmol electrons m^{-2}

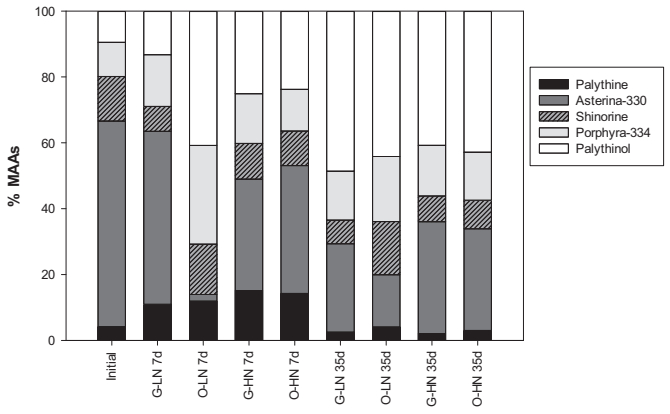

Fig. 10. Composition of MAAs expressed as the average of the percentage of each MAA type (palythine, asterina-330, shinorine, porhyra-334 or palythinol) related to the total MAA amounts in *G. cornea* at the beginning and after 7 and 35 days of cultivation under different experimental conditions: outdoor under high nitrogen (O-HN) or low nitrogen (O-LN) supply and indoor (greenhouse) under high nitrogen (G-HN) and low nitrogen (G-LN) supply. ($n = 3$).

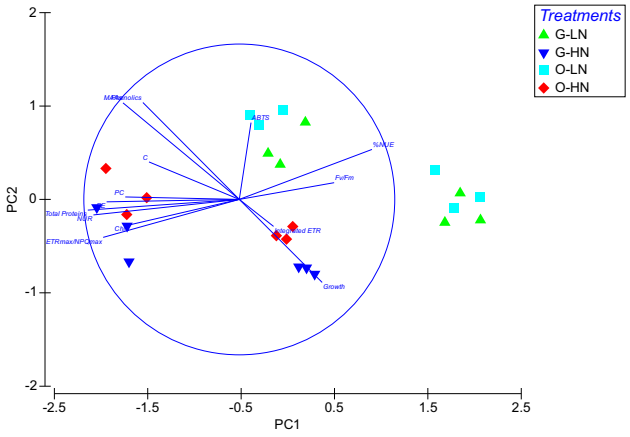

Fig. 11. Principal component analysis (PCA) of the different physiological variables measured in *G. cornea* cultivated under different experimental conditions: outdoor under high nutrient (O-HN) or low nutrient (O-LN) supply and indoor (greenhouse) under high nutrient (G-HN) and low nutrient (G-LN) supply. The following variables were considered in this analysis: growth rates, photosynthetic parameters (integrated ETR, F_v/F_m, ETR_{max}/NPQ_{max}), biofiltration parameters (NUE and NUR), bioactive compounds (total proteins, photosynthetic pigments chlorophyll *a* (Chl *a*), phycoerythrin (PE) and phycocyanin (PC), MAAs and Phenolic compounds), total internal carbon (C), and antioxidant capacity (ABTS). Data were log(x + 1) transformed before the analysis.

s^{-1}. These differences have been previously reported in the green macroalgae: *Ulva lactuca* (40 and 20 μmol electrons m^{-2} s^{-1} were obtained *in situ* and *ex situ*, respectively) [88], and *Ulva rigida* (60–93 and 9–33 μmol electrons m^{-2} s^{-1} *in situ* and *ex situ*, respectively) [89]. In the green microalgae, *Chlorella fusca*, those differences were also observed (560 and 250 μmol electrons m^{-2} s^{-1}, *in situ* and *ex situ*, respectively) [90]. A possible explanation is that under full solar radiation, more light was available to be utilized by accessory and essential photosynthetic pigments, which can also optimize the transferred photons to reaction center chlorophyll *a*, reaching a greater extent than artificial light as blue, red or halogen obtained from PAM-light sources.

Biomass and the accumulation of bioactive compounds are expected to be related to the photosynthetic capacity. Few studies have used ETR as estimator of biomass productivity [91]. Jerez et al. [90] showed a good correlation between biomass productivity (measured as dry weight) and estimated biomass productivity obtained from integrated daily ETR and its conversion in C and biomass in the green microalga *C. fusca* grown in outdoor thin layer cascade cultivators. Obata et al. [92] showed a linear relation between ETRr and Chl *a* in *Chlorella vulgaris* cultured under artificial light. Torzillo et al. [93] reported a good correlation between integrated daily ETR and biomass productivity in *Spirulina platensis* grown in outdoor photobioreactor. In this study, positive correlations between integrated ETR (calculated from different daily cycles), growth and biomass productivity were found. This result reinforces the relevance of integrated ETR as one of the most representative data possible to be obtained by using PAM fluorometry evaluating photosynthetic activity by using chlorophyll *a* fluorescence. However, efforts to conduct this measurement in an accurate way for a daily period by measuring in different periods of the day are still exhaustive. Automated monitoring alternatives could help in photosynthesis optimization measurements, and integrated ETR can be properly a good profit for estimating biomass productivity easily.

Morphological and color changes of the thalli were evident through the experimental period. Thalli grown under high nutrient levels and inside the green house (G-LN) were more reddish than the other ones. Thalli grown outdoor presented a brownish color as consequence of the variation in the pigments content ratios. After 35 days of culture, (PE + PC)/Chl *a* ratio of the algae cultured under HN was higher (9.03 and 8.60 under G and O treatments, respectively) than algae cultured in LN (5.90 (G) and 7.27 (O)). In addition of the color, thalli presented different morphology due to the treatment, *e.g.* thalli under O-HN presented more new growing branches, followed by G-HN than in the others treatments. These branches can increase the surface/volume (S/V), increasing the uptake of nutrients. The algal morphology after 35 days culture presented more spherical morphology, although the thallus filaments remained. These morphological changes including increased of S/V ratios of the thalli have been previously observed in the red algae *Asparagopsis armata* (*Falkenbergia rufolanosa*) grown in fishpond effluents [79,94] and other algal species [64]. The simpler morphologies as filaments with high S/V ratios were related to high nutrient uptake [95].

The different algal thallus colors related to different biochemical composition found in our experiment with *G. cornea* could have interest for culinary application. For example, the red alga *Chondrus crispus* (irish moss) produced for food by the Canadian company, Acadian Seaplants Ltd., sell in the market the combination of specimens of *C. crispus* of different colors (green, brownish o reddish), a highly appreciated product by the consumers [96]. So, brownish or reddish color variations can be properly obtained in association with efficient nutritional removal from the environment by cultivating *G. cornea*.

The maximal N productivity in *G. cornea* under HN treatments was 2gN m^{-2} d^{-1}. This value was higher than that reported in other algae as *U. rigida* (1.4gN m^{-2} d^{-1}) [83], *U. lactuca* (0.5 g N m^{-2} d^{-1}) [63], *Gracilaria conferta* (0.8 g N m^{-2} d^{-1}) [34], but lower to other species reported as biofilters, *A. armata* (2.7–5.9 g N m^{-2} d^{-1}) [84]. Gómez-Pinchetti et al. [97] reported higher N productivity in *G. cornea* than that in this study, *i.e.* 10.1 g N m^{-2} d^{-1} and 6.1 g N m^{-2} d^{-1} in algae cultivated outdoor and indoor respectively, by using tanks of 1500 L and 1.0 m of diameter. This difference can be explained by the use of higher algal density in bigger tanks (1500 L) compared to 90 L tanks used in this study.

The decrease of the biomass productivity of *G. cornea* through the time in spite of the increase of photosynthetic capacity (increased ETR) and incorporation of inorganic nitrogen, can be explained as the energy is being used in the accumulation of bioactive compounds and not in biomass production. In fact, NUR is correlated to the accumulation of photosynthetic pigments (Chl *a* and biliproteins), total proteins, MAAs, polyphenols and internal total C and N, in contrast to the negative correlation to these compounds and growth or biomass productivity.

Probably, the bioactive compounds accumulation was directly related to the production of ATP and NADPH by photosynthesis, *i.e.*, related to photosynthetic capacity (integrated ETR), ETR_{max}/NPQ_{max}

ratio, and to the nitrogen uptake rate (NUR). ETR_{max}/NPQ_{max} is the ratio between the energy used for the assimilation of carbon nitrogen through photosynthesis processes (expressed ad the maximal ETR) related to energy dissipated as heat no used in the electron transport chain (expressed as maximal NPQ). Thus, higher values represent a higher proportion of the energy higher used for photosynthetic production *i.e.* higher ATP, NADPH and consequently higher conversion of CO_2 in organic carbon or inorganic nitrogen to proteins.

Some high value compounds are related to secondary metabolism and they are produced under stress conditions, normally related to a decreasing in biomass productivity [98–100]. Thus, under full solar radiation and high nutrient level (O-HN), the highest levels of UV absorbing compounds and antioxidant molecules (*e.g.* MAAs and polyphenols) were reached, whereas the highest levels of Chl *a*, PE and PC, were reached under HN, but without UVR exposure (G-HN).

In general, the internal compounds increased throughout the experimental period, although differences among treatments were observed. Interestingly, several biocompounds were stimulated in a short-term period (7 days), whereas others were accumulated after a long period (35 days). The highest increase of N-compounds was produced, as expected, under HN treatments as phycobiliproteins, total proteins and MAAs, but also in non-N compounds as polyphenols. These three compounds present antioxidant and anti-inflammatory capacities, *i.e.* MAAs [101,102], polyphenols [103] and phycoerythrin [104,105]. Extracts of *G. cornea* have shown antioxidant, anti-inflammatory and immunomodulatory activities [62,106–108].

The accumulation of Chl *a* and phycobiliproteins under HN is an indicator of a good physiological status. Phycobiliproteins, in addition to accessory pigments, can act as N reservoir in red algae and they can be used under metabolic stress [109–114]. The low N availability reduce the content of Chl *a*, phycobiliproteins and proteins. As a consequence, Rubisco can also decrease and photosynthetic activity is depleted [115–117]. The proteolysis of phycobiliproteins can reach 17.3 % of soluble proteins in red algae providing aminoacids and microelements to the cells under nutrient limited conditions [110,118].

In this study, the level of total MAAs were 16 times higher under high nitrogen supply (HN) than under non-enriched seawater (LN). The level of MAAs presents a facultative pattern under laboratory conditions, *e.g.* the level of MAAs in seawater was 0.2 mg MAAs g^{-1} DW and after increasing the level of inorganic nitrogen and exposure to UVR, the level increased to 1 mg MAAs g^{-1} DW, an increment of 25 times [62,119]. MAAs protects PSII in species exposed to UVR, maintaining the photosynthetic capacity due to avoidance or reduction of UVR damage [120]. MAAs are accumulated under high nitrogen availability, thus N-NH_4^+ has a photoprotector role, due to both the increased photosynthetic capacity as by the accumulation of MAAs as it has been previously reported in *G. cornea* [121], other Gracilariales [26,34,61,122] and other red alga species as *Porphyra* spp. [46,47] or *A. armata* [79]. Thus, the highest accumulation of MAAs is produced under UVR and high inorganic nitrogen availability, reaching the maximal value of 5.1 mg MAAs g^{-1}DW, higher values of MAAs compared to other studies with the same species grown under lower nitrogen supply [121] but lower than the levels reached by species in the Order Bangiales [99,123,124]. A relation between NUR and MAAs accumulation has been previously reported in *G. cornea* (formerly *Hydropuntia cornea*) [70,121]. Under flux of 150 μM NH_4^+ h^{-1}, the available N is mainly used for the synthesis of MAAs as reported by Figueroa et al. [79]. Short-term variation on the MAAs composition has been reported in red macroalgae [62,125,126]. In this work, the levels of the different MAAs changes throughout the time being affected by light and nutrient treatments. The possible degradation or interconversion of the different MAAs can be related to the chemical characteristics of the amino acid radicals of the three main MAAs (palythinol, shinorine and Porphyra-334). These three MAAs present lower degradation rates when compared to others [127]. The increase of palythinol in *G. cornea* cultivated under solar radiation and high nitrogen level (O-HN) can be related by the high chemical stability of this MAA.

The PCA analysis also showed relationship between polyphenols and the level of nitrogen (positive correlation to NUR) and UVR as Person analysis showed. As have been found by other authors. Generally, polyphenols are produced under stress conditions and they are involved in photoprotection against UVR [128,129].

Gracilaria cornea is an algal species with developed culture techniques under IMTA conditions and the biomass is commercialized to produce agar in the Mexican Caribbean [60,130,131]. Thus, in addition of N-compounds as MAAs and phycobiliproteins, *G. cornea* biomass could also promise biomass to extract C-compounds as Agar. On the other hand, the biorefinery process can be applied to extract high value N compounds as MAAs and biliproteins followed to the extraction of agar under high temperature.

As it was mentioned above, the capacity to incorporate nutrients is one of the highest among different macroalgae [94,132,133]. Considering a biofiltration efficiency of 57 % and a high MAAs productivity, 113-253 mg MAAs m^{-2} d^{-1} (Fig. 9), according to the estimation of MAAs production in *Asparagospsis armata* under IMTA conditions (Figueroa et al., 2008), it would be possible to produce by culture *G. cornea* under IMTA conditions 19.7 T DW y^{-1} of algal biomass and 34.5 kg MAAs.

The high biomass and MAAs productivity found in this study to *G. cornea* suggests the use of this species to produce photoprotective compounds for the cosmetic industry. More precisely, MAAs are promising molecules with potential used in the cosmeceutical industry due to their UV screen properties and potential antioxidant activities. MAAs can protect against erythema, photoaging or immunosuppresion [134]. Diverse biological properties have been also described in MAAs during the last years, such as DNA protection, prevention of photoaging or anti-inflammatory capacity, among others [23,101,102,135–138]. As it is important to develop new materials as UV filters with higher termo-, photostability, biodegradability and no toxic effects, both for humans and the whole ecosystem. Many studies have suggested the use of MAAs as UV screen substances [23,102,139,140]. However, they have not yet been broadly exploited at commercial scale and only a few products are available such as Helioguard®365 or Helionori® with MAAs extracted from *Porphyra umbilicalis*.

5. Conclusions

Gracilaria cornea, intensively grown in tanks under solar radiation, is an efficient biofilter of inorganic nutrients. We have focused in this study the biofiltration on inorganic nitrogen compounds since we have studied the accumulation of high values nitrogen compounds as MAAS and phycobiliproteins. A high productivity and a good physiological state were observed in all treatments, especially with HN. The different treatments have affected the internal biochemical composition, mainly in the outdoor condition, accumulating different bioactive compounds such as MAAs, polyphenols or biliproteins with potential nutraceutical and cosmeceutical applications. MAAs content increased over the experimental period, mainly in the O-HN treatment reaching values of 5.1 ± 0.47 mg g^{-1} DW. MAAs are potential candidates to be used as biological UV-filters, as they are natural compounds without reported toxicity and high photo- and thermostability. Thus, high levels of UV photoprotectors could be obtained from *G. cornea* biomass grown under high nutrients simulating nutrient levels under IMTA conditions. Future experiments by using fish pond effluents has to be conducted since under IMTA not only it is necessary to be into account nutrient conditions but also other features as low pH and dissolved oxygen, associated bacteria and levels dissolved organic carbon among others.

CRediT authorship contribution statement

Félix L. Figueroa: Conceptualization, Methodology, Investigation, Writing – original draft, Writing – review & editing, Supervision,

Funding acquisition. **Félix Álvarez-Gómez:** Conceptualization, Methodology, Formal analysis, Investigation, Resources, Data curation, Writing – original draft, Writing – review & editing. **José Bonomi-Barufi:** Formal analysis, Investigation, Writing – original draft, Writing – review & editing. **Julia Vega:** Formal analysis, Investigation, Writing – original draft, Writing – review & editing. **Thais F. Massocato:** Formal analysis, Investigation, Writing – original draft, Writing – review & editing. **Juan Luis Gómez-Pinchetti:** Conceptualization, Methodology, Resources, Writing – review & editing, Supervision, Funding acquisition. **Nathalie Korbee:** Conceptualization, Methodology, Formal analysis, Investigation, Writing – original draft, Writing – review & editing, Supervision.

Declaration of competing interest

This manuscript has not any conflict of interest.

Data availability

Data will be made available on request.

Acknowledgements

This study was financed by resources of the Photobiology and Biotechnology of aquatic organisms (FYBOA-RNM 295) research group and the Project "Photoprotectors of marine algae: compatible cosmeceutics to the ocean" (UMA18-FEDER JA-162) and Nazca Project (P20-00458) of the Andalusian Goverment. Funding for open access charge: Universidad de Málaga / CBUA. Special thanks to Demetrio Cruz Lozano for the design and creation of Fig. 1 of this work.

Appendix A. Supplementary data

Supplementary data to this article can be found online at https://doi.org/10.1016/j.algal.2022.102890.

References

[1] B.S. Halpern, S. Walbridge, K.A. Selkoe, C.V. Kappel, F. Micheli, C. D'Agrosa, J. F. Bruno, K.S. Casey, C. Ebert, H.E. Fox, R. Fujita, D. Heinemann, H.S. Lenihan, E. M.P. Madin, M.T. Perry, E.R. Selig, M. Spalding, R. Steneck, R. Watson, A global map of human impact on marine ecosystems, Science 319 (2008) 948–952, https://doi.org/10.1126/science.1149345.

[2] G. Chen, H. Shi, J. Tao, L. Chen, Y. Liu, G. Lei, X. Liu, J.P. Smol, Industrial arsenic contamination causes catastrophic changes in freshwater ecosystems, Sci. Rep. 5 (2015) 1–7, https://doi.org/10.1038/srep17419.

[3] L. Paruch, A.M. Paruch, H.G. Eiken, R. Sørheim, Faecal pollution affects abundance and diversity of aquatic microbial community in anthropo-zoogenically influenced lotic ecosystems, Sci. Rep. 9 (2019) 1–13, https://doi.org/10.1038/s41598-019-56058-x.

[4] B. Worm, E.B. Barbier, N. Beaumont, J.E. Duffy, C. Folke, B.S. Halpern, J.B. C. Jackson, H.K. Lotze, F. Micheli, S.R. Palumbi, E. Sala, K.A. Selkoe, J. J. Stachowicz, R. Watson, Impacts of biodiversity loss on ocean ecosystem services, Science 314 (2006) 787–790, https://doi.org/10.1126/SCIENCE.1132294.

[5] B. Worm, H.K. Lotze, Effects of eutrophication, grazing, and algal blooms on rocky shores, Limnol. Oceanogr. 51 (2006) 569–579, https://doi.org/10.4319/LO.2006.51.1_PART_2.0569.

[6] K. Brander, Impacts of climate change on fisheries, J. Mar. Syst. 79 (2010) 389–402, https://doi.org/10.1016/J.JMARSYS.2008.12.015.

[7] A. Neori, T. Chopin, M. Troell, A.H. Buschmann, G.P. Kraemer, C. Halling, M. Shpigel, C. Yarish, Integrated aquaculture: rationale, evolution and state of the art emphasizing seaweed biofiltration in modern mariculture, Aquaculture 231 (2004) 361–391, https://doi.org/10.1016/J.AQUACULTURE.2003.11.015.

[8] A.H. Buschmann, C. Camus, J. Infante, A. Neori, Á. Israel, M.C. Hernández-González, S.V. Pereda, J.L. Gomez-Pinchetti, A. Golberg, N. Tadmor-Shalev, A. T. Critchley, Seaweed production: overview of the global state of exploitation, farming and emerging research activity, Eur. J. Phycol. 52 (2017) 391–406, https://doi.org/10.1080/09670262.2017.1365175.

[9] A.H. Buschmann, J.A. Correa, R. Westermeier, R. Norambuena, M.del C. Hernández-González, Red algal farming in Chile: a review, Aquaculture 194 (2001) 203–220, https://doi.org/10.1016/S0044-8486(00)00518-4.

[10] M. Troell, C. Halling, A. Neori, T. Chopin, A.H. Buschmann, N. Kautsky, C. Yarish, Integrated mariculture: asking the right questions, Aquaculture 226 (2003) 69–90, https://doi.org/10.1016/S0044-8486(03)00469-1.

[11] D. Robledo, L. Navarro-Angulo, D.V. Lozano, Y. Freile-Pelegrín, Nutrient removal efficiency of Hydropuntia cornea in an integrated closed recirculation system with pink shrimp Farfantepenaeus brasiliensis, Aquac. Res. 45 (2014) 1648–1658, https://doi.org/10.1111/ARE.12111.

[12] I. Hernández, M.A. Fernández-Engo, J.L. Pérez-Lloréns, J.J. Vergara, Integrated outdoor culture of two estuarine macroalgae as biofilters for dissolved nutrients from Sparus auratus waste waters, J. Appl. Phycol. 17 (2005) 557–567, https://doi.org/10.1007/s10811-005-9006-6.

[13] I. Hernández, A. Pérez-Pastor, J.J. Vergara, J.F. Martínez-Aragón, M.Á. Fernández-Engo, J.L. Pérez-Lloréns, Studies on the biofiltration capacity of Gracilariopsis longissima: from microscale to macroscale, Aquaculture 252 (2006) 43–53, https://doi.org/10.1016/J.AQUACULTURE.2005.11.048.

[14] A. Neori, M. Troell, T. Chopin, C. Yarish, A. Critchley, A.H. Buschmann, Environment: science and policy for sustainable development the need for a balanced ecosystem approach to blue revolution, Aquaculture (2007), https://doi.org/10.3200/ENVT.49.3.36-43.

[15] M.H. Abreu, R. Pereira, C. Yarish, A.H. Buschmann, I. Sousa-Pinto, IMTA with Gracilaria vermiculophylla: productivity and nutrient removal performance of the seaweed in a land-based pilot scale system, Aquaculture 312 (2011) 77–87, https://doi.org/10.1016/J.AQUACULTURE.2010.12.036.

[16] V.K. Dhargalkar, X.N. Verlecar, Southern Ocean seaweeds: a resource for exploration in food and drugs, Aquaculture 287 (2009) 229–242, https://doi.org/10.1016/J.AQUACULTURE.2008.11.013.

[17] S.L. Holdt, S. Kraan, Bioactive compounds in seaweed: functional food applications and legislation, J. Appl. Phycol. 23 (2011) 543–597, https://doi.org/10.1007/s10811-010-9632-5.

[18] R. Gade, M. Siva Tulasi, V. Aruna Bhai, Seaweeds: a novel biomaterial, Int. J. Pharm. Pharm. Sci. 5 (2013) 40–44.

[19] A. Ullah, S. Heng, M.F.H. Munis, S. Fahad, X. Yang, Phytoremediation of heavy metals assisted by plant growth promoting (PGP) bacteria: a review, Environ. Exp. Bot. 117 (2015) 28–40, https://doi.org/10.1016/J.ENVEXPBOT.2015.05.001.

[20] A. Robin, P. Chavel, A. Chemodanov, A. Israel, A. Golberg, Diversity of monosaccharides in marine macroalgae from the eastern Mediterranean Sea, Algal Res. 28 (2017) 118–127, https://doi.org/10.1016/J.ALGAL.2017.10.005.

[21] G. Gao, J.G. Burgess, M. Wu, S. Wang, K. Gao, Using macroalgae as biofuel: current opportunities and challenges, Bot. Mar. 63 (2020) 355–370, https://doi.org/10.1515/bot-2019-0065.

[22] L.A. Tziveleka, E. Ioannou, V. Roussis, Ulvan, a bioactive marine sulphated polysaccharide as a key constituent of hybrid biomaterials: a review, Carbohydr. Polym. 218 (2019) 355–370, https://doi.org/10.1016/J.CARBPOL.2019.04.074.

[23] J. Vega, G. Schneider, B.R. Moreira, C. Herrera, J. Bonomi-Barufi, F.L. Figueroa, Mycosporine-like amino acids from red macroalgae: UV-photoprotectors with potential cosmeceutical applications, Appl. Sci. 5112 (2021) 5112, https://doi.org/10.3390/APP11115112.

[24] C. Peteiro, N. Sánchez, B. Martínez, Mariculture of the asian kelp undaria pinnatifida and the native kelp saccharina latissima along the Atlantic coast of southern Europe: an overview, Algal Res. 15 (2016) 9–23, https://doi.org/10.1016/J.ALGAL.2016.01.012.

[25] G. Gao, L. Gao, Q. Fu, X. Li, J. Xu, Coculture of the Pacific white shrimp Litopenaeus vannamei and the macroalga Ulva linza enhances their growth rates and functional properties, J. Clean. Prod. 349 (2022), 131407, https://doi.org/10.1016/j.jclepro.2022.131407.

[26] J.B. Barufi, N. Korbee-Peinado, M.C. Oliveira, F.L. Figueroa, Effects of N supply on the accumulation of photosynthetic pigments and photoprotectors in Gracilaria tenuistipitata (Rhodophyta) cultured under UV radiation, J. Appl. Phycol. 23 (2011) 457–466, https://doi.org/10.1007/s10811-010-9603-x.

[27] F. Figueroa, J.Bonomi Barufi, E. Malta, R. Conde-Álvarez, U. Nitschke, F. Arenas, M. Mata, S. Connan, M. Abreu, R. Marquardt, F. Vaz-Pinto, T. Konotchick, P. Celis-Plá, M. Hermoso, G. Ordoñez, E. Ruiz, P. Flores, J. de los Ríos, D. Kirke, F. Chow, C. Nassar, D. Robledo, Á. Pérez-Ruzafa, E. Bañares-España, M. Altamirano, C. Jiménez, N. Korbee, K. Bischof, D. Stengel, Short-term effects of increasing CO2, nitrate and temperature on three Mediterranean macroalgae: biochemical composition, Aquat. Biol. 22 (2014) 177–193, https://doi.org/10.3354/ab00610.

[28] G. Williamson, C.D. Kay, A. Crozier, The bioavailability, transport, and bioactivity of dietary flavonoids: a review from a historical perspective, Compr. Rev. Food Sci. Food Saf. 17 (2018) 1054–1112, https://doi.org/10.1111/1541-4337.12351.

[29] F. Álvarez-Gómez, Z.L. Bouzon, N. Korbee, P. Celis-Plá, C. Schmidt, F.L. Figueroa, Combined effects of UVR and nutrients on cell ultrastructure, photosynthesis and biochemistry in Gracilariopsis longissima (Gracilariales, Rhodophyta), Algal Res. 26 (2017) 190–202, https://doi.org/10.1016/j.algal.2017.07.022.

[30] G. Schneider, F.L. Figueroa, J. Vega, A. Avilés, P. Chaves, P.A. Horta, N. Korbee, J. Bonomi-Barufi, Physiological and biochemical responses driven by different UV-visible radiation in: Osmundea pinnatifida (Hudson) Stackhouse (Rhodophyta), Photochem. Photobiol. Sci. 19 (2020) 1650–1664, https://doi.org/10.1039/d0pp00135j.

[31] W.C. Dunlap, J.M. Shick, REVIEW—ULTRAVIOLET radiation-absorbing mycosporine-like amino acids in CORAL reef organisms: a biochemical and environmental perspective, J. Phycol. 34 (1998) 418–430, https://doi.org/10.1046/J.1529-8817.1998.340418.X.

[32] J.I. Carreto, M.O. Carignan, Mycosporine-like amino acids: relevant secondary metabolites. Chemical and ecological aspects, Mar. Drugs 9 (2011) 387–446, https://doi.org/10.3390/md9030387.
[33] P. Huovinen, J. Matos, I.S. Pinto, F.L. Figueroa, The role of ammonium in photoprotection against high irradiance in the red alga Grateloupia lanceola, Aquat. Bot. 84 (2006) 308–316, https://doi.org/10.1016/j.aquabot.2005.12.002.
[34] F.L. Figueroa, A. Israel, A. Neori, B. Martínez, E.J. Malta, A. Put, S. Inken, R. Marquardt, R. Abdala, N. Korbee, Effect of nutrient supply on photosynthesis and pigmentation to short-term stress (UV radiation) in Gracilaria conferta (Rhodophyta), Mar. Pollut. Bull. 60 (2010) 1768–1778, https://doi.org/10.1016/j.marpolbul.2010.06.009.
[35] F. Álvarez-Gómez, N. Korbee, V. Casas-Arrojo, R.T. Abdala-Díaz, F.L. Figueroa, UV photoprotection, cytotoxicity and immunology capacity of red algae extracts, Molecules 24 (2019) 341, https://doi.org/10.3390/molecules24020341.
[36] C.F. D'Elia, J.A. DeBoer, Nutritional studies of two red algae. ii. kinetics of ammonium and nitrate uptake, J. Phycol. 14 (1978) 266–272, https://doi.org/10.1111/j.1529-8817.1978.tb00297.x.
[37] J.A. DeBoer, J.H. Ryther, Potential yields from a waste-recycling algal mariculture system, Mar. Plant Biomass Pacific Northwest Coast. (1977) 231–248.
[38] A. Israel, J. Gavrieli, A. Glazer, M. Friedlander, Utilization of flue gas from a power plant for tank cultivation of the red seaweed Gracilaria cornea, Aquaculture 249 (2005) 311–316, https://doi.org/10.1016/J.AQUACULTURE.2005.04.058.
[39] W.H. Zuldin, S. Yassir, R. Shapawi, Growth and biochemical composition of Kappaphycus (Rhodophyta) in customized tank culture system, J. Appl. Phycol. 28 (2016) 2453–2458, https://doi.org/10.1007/S10811-016-0792-9.
[40] F.L. Figueroa, A. Bueno, N. Korbee, R. Santos, L. Mata, A. Schuenhoff, Accumulation of mycosporine-like amino acids in Asparagopsis armata grown in tanks with fishpond effluents of gilthead sea bream, Sparus aurata, J. World Aquac. Soc. 39 (2008) 692–699, https://doi.org/10.1111/j.1749-7345.2008.00199.x.
[41] S.K. Kim, Y.D. Ravichandran, S.B. Khan, Y.T. Kim, Prospective of the cosmeceuticals derived from marine organisms, biotechnol, Bioprocess Eng. 13 (2008) 511–523, https://doi.org/10.1007/s12257-008-0113-5.
[42] B.E. Lapointe, L.D. Williams, J.C. Goldman, J.H. Ryther, The mass outdoor culture of macroscopic marine algae, Aquaculture 8 (1976) 9–21, https://doi.org/10.1016/0044-8486(76)90015-6.
[43] J.B. Barufi, M.T. Mata, M.C. Oliveira, F.L. Figueroa, Nitrate reduces the negative effect of UV radiation on photosynthesis and pigmentation in Gracilaria tenuistipitata (Rhodophyta): the photoprotection role of mycosporine-like amino acids, Phycologia 51 (2012) 636–648, https://doi.org/10.2216/10.77.1.
[44] M.L. Cornish, D.J. Garbary, Antioxidants from macroalgae: potential applications in human health and nutrition, Algae 25 (2010) 155–171, https://doi.org/10.4490/algae.2010.25.4.155.
[45] D.B. Stengel, S. Connan, Z.A. Popper, Algal chemodiversity and bioactivity: sources of natural variability and implications for commercial application, Biotechnol. Adv. 29 (2011) 483–501, https://doi.org/10.1016/J.BIOTECHADV.2011.05.016.
[46] N. Korbee, P. Huovinen, F.L. Figueroa, J. Aguilera, U. Karsten, Availability of ammonium influences photosynthesis and the accumulation of mycosporine-like amino acids in two porphyra species (Bangiales, Rhodophyta), Mar. Biol. 146 (2005) 645–654, https://doi.org/10.1007/s00227-004-1484-6.
[47] N. Korbee-Peinado, R.T. Abdala Díaz, F.L. Figueroa, E.W. Helbling, Ammonium and UV radiation stimulate the accumulation of mycosporine-like amino acids in Porphyra columbina (Rhodophyta) from Patagonia, Argentina, J. Phycol. 40 (2004) 248–259, https://doi.org/10.1046/j.1529-8817.2004.03013.x.
[48] F. Álvarez-Gómez, Z.L. Bouzon, N. Korbee, P. Celis-Plá, C. Schmidt, F.L. Figueroa, Combined effects of UVR and nutrients on cell ultrastructure, photosynthesis and biochemistry in Gracilariopsis longissima (Gracilariales, Rhodophyta), Algal Res. 26 (2017) 190–202, https://doi.org/10.1016/j.algal.2017.07.022.
[49] F.L. Figueroa N. Korbee F. de la Coba C. Gil Jerez J. Bonomi Barufi L. Güenaga Unzetabarrenechea J.L. Gómez-Pinchetti M.H. Abreu R. Pereira I. Sousa-Pinto Valorización de la biomasa de macroalgas en acuicultura multitrófica integrada (AMTI): aplicaciones en cosmética y nutraceútica (fotoprotectores y antioxidantes),n.d.
[50] M.S. Bansemer, J.G. Qin, J.O. Harris, D.N. Duong, K.-L. Currie, G.S. Howarth, D. A.J. Stone, Dietary inclusions of dried macroalgae meal in formulated diets improve the growth of greenlip abalone (Haliotis laevigata), J. Appl. Phycol. 28 (2016) 3645–3658, https://doi.org/10.1007/S10811-016-0829-0.
[51] L.M.P. Valente, M. Araújo, S. Batista, M.J. Peixoto, I. Sousa-Pinto, V. Brotas, L. M. Cunha, P. Rema, Carotenoid deposition, flesh quality and immunological response of Nile tilapia fed increasing levels of IMTA-cultivated ulva spp, J. Appl. Phycol. 28 (2016) 691–701, https://doi.org/10.1007/s10811-015-0590-9.
[52] A.J. Vizcaíno, S.I. Mendes, J.L. Varela, I. Ruiz-Jarabo, R. Rico, F.L. Figueroa, R. Abdala, M.Á. Moriñigo, J.M. Mancera, F.J. Alarcón, Growth, tissue metabolites and digestive functionality in Sparus aurata juveniles fed different levels of macroalgae, Gracilaria cornea and Ulva rigida, Aquac. Res. 47 (2016) 3224–3238, https://doi.org/10.1111/ARE.12774.
[53] M. Shpigel, L. Guttman, L. Shauli, V. Odintsov, D. Ben-Ezra, S. Harpaz, Ulva lactuca from an integrated multi-trophic aquaculture (IMTA) biofilter system as a protein supplement in gilthead seabream (Sparus aurata) diet, Aquaculture 481 (2017) 112–118, https://doi.org/10.1016/j.aquaculture.2017.08.006.
[54] M. Araújo, P. Rema, I. Sousa-Pinto, L.M. Cunha, M.J. Peixoto, M.A. Pires, F. Seixas, V. Brotas, C. Beltrán, L.M.P. Valente, Dietary inclusion of IMTA-cultivated Gracilaria vermiculophylla in rainbow trout (Oncorhynchus mykiss) diets: effects on growth, intestinal morphology, tissue pigmentation, and immunological response, J. Appl. Phycol. 28 (2016) 679–689, https://doi.org/10.1007/s10811-015-0591-8.
[55] J.L. Pérez-Lloréns, I. Hernández, J.J. Vergara, F.G. Brun, A. León, ¿Las Algas se Comen ? Un Periplo por la Biología , la Historia , las Curiosidades y la Gastronomía, Universidad de Cádiz, 2016.
[56] R.M. Hernández-Herrera, F. Santacruz-Ruvalcaba, J. Zañudo-Hernández, G. Hernández-Carmona, Activity of seaweed extracts and polysaccharide-enriched extracts from Ulva lactuca and Padina gymnospora as growth promoters of tomato and mung bean plants, J. Appl. Phycol. 28 (2016) 2549–2560, https://doi.org/10.1007/S10811-015-0781-4.
[57] W. Khan, U.P. Rayirath, S. Subramanian, M.N. Jithesh, P. Rayorath, D.M. Hodges, A.T. Critchley, J.S. Craigie, J. Norrie, B. Prithiviraj, Seaweed extracts as biostimulants of plant growth and development, J. Plant Growth Regul. 28 (2009) 386–399, https://doi.org/10.1007/S00344-009-9103-X.
[58] J.F. Martínez-Aragón, I. Hernández, J.L. Pérez-Lloréns, R. Vázquez, J.J. Vergara, Biofiltering efficiency in removal of dissolved nutrients by three species of estuarine macroalgae cultivated with sea bass (Dicentrarchus labrax) waste waters 1. Phosphate, J. Appl. Phycol. 145 (14) (2002) 365–374, https://doi.org/10.1023/A:1022134701273, 2002.
[59] L. Mata, J. Silva, A. Schuenhoff, R. Santos, Is the tetrasporophyte of Asparagopsis armata (Bonnemaisoniales) limited by inorganic carbon in integrated aquaculture?1, J. Phycol. 43 (2007) 1252–1258, https://doi.org/10.1111/J.1529-8817.2007.00421.X.
[60] F.L. Figueroa, N. Korbee, R. Abdala, C.G. Jerez, M. López-de la Torre, L. Güenaga, M.A. Larrubia, J.L. Gómez-Pinchetti, Biofiltration of fishpond effluents and accumulation of N-compounds (phycobiliproteins and mycosporine-like amino acids) versus C-compounds (polysaccharides) in Hydropuntia cornea (Rhodophyta), Mar. Pollut. Bull. 64 (2012) 310–318, https://doi.org/10.1016/j.marpolbul.2011.11.012.
[61] M. Barceló-Villalobos, F.L. Figueroa, N. Korbee, F. Álvarez-Gómez, M.H. Abreu, Production of mycosporine-like amino acids from Gracilaria vermiculophylla (Rhodophyta) cultured through one year in an integrated multi-trophic aquaculture (IMTA) system, Mar. Biotechnol. 19 (2017) 246–254, https://doi.org/10.1007/s10126-017-9746-8.
[62] F. Álvarez-Gómez, N. Korbee, F.L. Figueroa, Effects of UV radiation on photosynthesis, antioxidant capacity and the accumulation of bioactive compounds in Gracilariopsis longissima, Hydropuntia cornea and halopithys incurva (Rhodophyta), J. Phycol. 55 (2019) 1258–1273, https://doi.org/10.1111/jpy.12899.
[63] F.L. Figueroa, A. Israel, A. Neori, B. Martínez, E.Jan Malta, P. Ang, S. Inken, R. Marquardt, N. Korbee, Effects of nutrient supply on photosynthesis and pigmentation in Ulva lactuca (Chlorophyta): responses to short-term stress, Aquat. Biol. 7 (2009) 173–183, https://doi.org/10.3354/ab00187.
[64] J. Vega, F. Álvarez-Gómez, L. Güenaga, F.L. Figueroa, J.L. Gómez-Pinchetti, Antioxidant activity of extracts from marine macroalgae, wild-collected and cultivated, in an integrated multi-trophic aquaculture system, Aquaculture 522 (2020), 735088, https://doi.org/10.1016/j.aquaculture.2020.735088.
[65] P.S.M. Celis-Plá, N. Korbee, A. Gómez-Garreta, F.L. Figueroa, F.L. Figueroa, Seasonal photoacclimation patterns in the intertidal macroalga Cystoseira tamariscifolia (Ochrophyta), Sci. Mar. 78 (2014) 377–388, https://doi.org/10.3989/scimar.04053.05A.
[66] N.P. Navarro, A. Mansilla, F.L. Figueroa, N. Korbee, J. Jofre, E. Plastino, Short-term effects of solar UV radiation and NO3- supply on the accumulation of mycosporine-like amino acids in pyropia columbina (Bangiales, Rhodophyta) under spring ozone depletion in the sub-Antarctic region, Chile, Bot. Mar. 57 (2014) 9–20, https://doi.org/10.1515/bot-2013-0090.
[67] M. Jiménez del Río, Z. Ramazanov, G. García-Reina, Ulva rigida (Ulvales, Chlorophyta) tank culture as biofilters for dissolved inorganic nitrogen from fishpond effluents, Hydrobiologia 326 (1996) 61–66, https://doi.org/10.1007/BF00047787.
[68] T.R. Parsons, Y. Maita, C.M. Lalli, A Manual of Chemical & Biological Methods for Seawater Analysis, Elsevier, 1984, https://doi.org/10.1016/c2009-0-07774-5.
[69] F.L. Figueroa, R. Santos, R. Conde-Álvarez, L. Mata, J.L. Gómez Pinchetti, J. Matos, P. Huovinen, A. Schuenhoff, J. Silva, The use of chlorophyll fluorescence for monitoring photosynthetic condition of two tank-cultivated red macroalgae using fishpond effluents, Bot. Mar. 49 (2006) 275–282, https://doi.org/10.1515/BOT.2006.035.
[70] F.L. Figueroa, L. Escassi, E. Pérez-Rodríguez, N. Korbee, A.D. Giles, G. Johnsen, Effects of short-term irradiation on photoinhibition and accumulation of mycosporine-like amino acids in sun and shade species of the red algal genus Porphyra, J. Photochem. Photobiol. B Biol. 69 (2003) 21–30, https://doi.org/10.1016/S1011-1344(02)00388-3.
[71] P.H.C. Eilers, J.C.H. Peeters, A model for the relationship between light intensity and the rate of photosynthesis in phytoplankton, Ecol. Model. 42 (1988) 199–215, https://doi.org/10.1016/0304-3800(88)90057-9.
[72] A.R. Wellburn, The spectral determination of chlorophylls a and b, as well as total carotenoids, using various solvents with spectrophotometers of different resolution, J. Plant Physiol. 144 (1994) 307–313, https://doi.org/10.1016/S0176-1617(11)81192-2.
[73] P. Sampath-Wiley, C.D. Neefus, L.S. Jahnke, Seasonal effects of sun exposure and emersion on intertidal seaweed physiology: Fluctuations in antioxidant contents, photosynthetic pigments and photosynthetic efficiency in the red alga Porphyra umbilicalis Kützing (Rhodophyta, Bangiales), J. Exp. Mar. Biol. Ecol. 361 (2008) 83–91, https://doi.org/10.1016/J.JEMBE.2008.05.001.

[74] S.O. Lourenço, E. Barbarino, J.C. De-Paula, L.O.D.S. Pereira, U.M. Lanfer Marquez, Amino acid composition, protein content and calculation of nitrogen-to-protein conversion factors for 19 tropical seaweeds, Phycol. Res. 50 (2002) 233–241, https://doi.org/10.1046/j.1440-1835.2002.00278.x.
[75] O. Folin, V. Ciocalteu, On tyrosine and tryptophane determinations in proteins, J. Biol. Chem. 73 (1927) 627–650.
[76] U. Karsten, T. Sawall, D. Hanelt, K. Bischof, F.L. Figueroa, A. Flores-Moya, C. Wiencke, An inventory of UV-absorbing mycosporine-like amino acids in macroalgae from polar to warm-temperate regions, Bot. Mar. 41 (1998) 443–453, https://doi.org/10.1515/botm.1998.41.1-6.443.
[77] R. Re, N. Pellegrini, A. Proteggente, A. Pannala, M. Yang, C. Rice-Evans, Antioxidant activity applying an improved ABTS radical cation decolorization assay, Free Radic. Biol. Med. 26 (1999) 1231–1237, https://doi.org/10.1016/S0891-5849(98)00315-3.
[78] R. Rabiei, S.M. Phang, P.E. Lim, A. Salleh, J. Sohrabipour, D. Ajdari, G. A. Zarshenas, Productivity,Biochemical Composition and Biofiltering Performance of Agarophytic Seaweed,Gelidium Elegans (Red Algae) Grown in Shrimp Hatchery Effluents in Malaysia, 2016 https://aquadocs.org/handle/1834/11917.
[79] F.L. Figueroa, A. Bueno, N. Korbee, R. Santos, L. Mata, A. Schuenhoff, Accumulation of Mycosporine-like Amino Acids in Asparagopsis armata Grown in Tanks with Fishpond Effluents of Gilthead Sea Bream, Sparus aurata, J. World Aquac. Soc. 39 (2008) 692–699, https://doi.org/10.1111/j.1749-7345.2008.00199.x.
[80] R. Pereira, C. Yarish, A.T. Critchley, Seaweed aquaculture for human foods in land-based and IMTA systems, Sustain. FoodProd. (2013) 1405–1424, https://doi.org/10.1007/978-1-4614-5797-8_189.
[81] T. Ben-Ari, A. Neori, D. Ben-Ezra, L. Shauli, V. Odintsov, M. Shpigel, Management of Ulva lactuca as a biofilter of mariculture effluents in IMTA system, Aquaculture 434 (2014) 493–498, https://doi.org/10.1016/J.AQUACULTURE.2014.08.034.
[82] D.Y. Ashkenazi, A. Israel, A. Abelson, A novel two-stage seaweed integrated multi-trophic aquaculture, Rev. Aquac. 11 (2019) 246–262, https://doi.org/10.1111/RAQ.12238.
[83] L. Mata, R. Santos, Cultivation of Ulva rotundata (Ulvales, Chlorophyta) in raceways using semi-intensive fishpond effluents: yield and biofiltration, in: Proc. 17th Int. Seaweed Symp. Cape Town, South Africa, 28 January-2 Febr. 2001, 2003, pp. 237–242.
[84] A. Schuenhoff, L. Mata, R. Santos, The tetrasporophyte of Asparagopsis armata as a novel seaweed biofilter, Aquaculture 252 (2006) 3–11, https://doi.org/10.1016/J.AQUACULTURE.2005.11.044.
[85] D.B. Largo, A.G. Diola, M.S. Marababol, Development of an integrated multi-trophic aquaculture (IMTA) system for tropical marine species in southern cebu, Central Philippines, Aquac. Rep. 3 (2016) 67–76, https://doi.org/10.1016/j.aqrep.2015.12.006.
[86] M.A.J. Nederlof, A. Neori, M.C.J. Verdegem, A.C. Smaal, H.M. Jansen, Ulva spp. performance and biomitigation potential under high nutrient concentrations: implications for recirculating IMTA systems, J. Appl. Phycol. 34 (2022) 2157–2171, https://doi.org/10.1007/s10811-022-02751-w.
[87] F.L. Figueroa, B. Domínguez-González, N. Korbee, Vulnerability and acclimation to increased UVB radiation in three intertidal macroalgae of different morpho-functional groups, Mar. Environ. Res. 97 (2014) 30–38, https://doi.org/10.1016/j.marenvres.2014.01.009.
[88] B.J. Longstaff, T. Kildea, J.W. Runcie, A. Cheshire, W.C. Dennison, C. Hurd, T. Kana, J.A. Raven, A.W.D. Larkum, An in situ study of photosynthetic oxygen exchange and electron transport rate in the marine macroalga Ulva lactuca (Chlorophyta), Photosynth. Res. 74 (2002) 281–293, https://doi.org/10.1023/A:1021279627409.
[89] F.L. Figueroa, J. Bonomi-Barufi, P.S.M. Celis-Plá, U. Nitschke, F. Arenas, S. Connan, M.H. Abreu, E.-J. Malta, R. Conde-Álvarez, F. Chow, M.T. Mata, O. Meyerhoff, D. Robledo, D.B. Stengel, Short-term effects of increased CO2, nitrate and temperature on photosynthetic activity in Ulva rigida (Chlorophyta) estimated by different pulse amplitude modulated fluorometers and oxygen evolution, J. Exp. Bot. 72 (2021) 491–509, https://doi.org/10.1093/jxb/eraa473.
[90] C.G. Jerez, J.R. Malapascua, M. Sergejevová, J. Masojídek, F.L. Figueroa, Chlorella fusca (Chlorophyta) grown in thin-layer cascades: Estimation of biomass productivity by in-vivo chlorophyll a fluorescence monitoring, Algal Res. 17 (2016) 21–30, https://doi.org/10.1016/J.ALGAL.2016.04.010.
[91] J.W. Runcie, M.J. Riddle, Estimating primary productivity of marine macroalgae in East Antarctica using in situ fluorometry, Eur. J. Phycol. 47 (2012) 449–460, https://doi.org/10.1080/09670262.2012.736535.
[92] M. Obata, T. Toda, S. Taguchi, Using chlorophyll fluorescence to monitor yields of microalgal production, J. Appl. Phycol. 21 (2008) 315–319, https://doi.org/10.1007/S10811-008-9369-6.
[93] G. Torzillo, P. Bernardini, J. Masojídek, On-line monitoring of chlorophyll fluorescence to assess the extent of photoinhibition of photosynthesis induced by high oxygen concentration and low temperature and its effect on the productivity of outdoor cultures of Spirulina platensis (cyanobacteria), J. Phycol. 34 (1998) 504–510, https://doi.org/10.1046/J.1529-8817.1998.340504.X.
[94] L. Mata, H. Gaspar, F. Justino, R. Santos, Effects of hydrogen peroxide on the content of major volatile halogenated compounds in the red alga Asparagopsis taxiformis (Bonnemaisoniaceae), J. Appl. Phycol. 23 (2010) 827–832, https://doi.org/10.1007/S10811-010-9582-Y.
[95] R. Taylor, J. Peek, T. Rees, Scaling of ammonium uptake by seaweeds to surface area:volume ratio:geographical variation and the role of uptake by passive diffusion, Mar. Ecol. Prog. Ser. 169 (1998) 143–148, https://doi.org/10.3354/meps169143.
[96] J.S. Craigie, M.L. Cornish, L.E. Deveau, Commercialization of Irish moss aquaculture: the Canadian experience, Bot. Mar. 62 (2019) 411–432, https://doi.org/10.1515/BOT-2019-0017.
[97] J.L. Gómez-Pinchetti, S.Suárez Alvarez, A.Martel Quintana, G.García Reina, Alternative high-value seaweed species as biofilters for the purification of N–NH4 + enriched fishpond effluents, in: Algal Biotechnol. A Sea Oppor 267, 2002.
[98] K.K. Sharma, H. Schuhmann, P.M. Schenk, High lipid induction in microalgae for biodiesel production, Energies 5 (2012) 1532–1553, https://doi.org/10.3390/EN5051532, 5 (2012) 1532–1553.
[99] N. Navarro, F.L. Figueroa, N. Korbee, J. Bonomi, F.Á. Gómez, F. de la Coba, Mycosporine-like amino acids from red algae to develop natural UV sunscreens, in: R.P. Rastogi (Ed.), Sunscreens Source, Formul. Effic. Recomm, 2018, pp. 99–129.
[100] T.A. Rearte, F.L. Figueroa, C. Gómez-Serrano, C.G. Vélez, S. Marsili, C. V. González-López, M.C. Cerón-García, R.T. Abdala-Díaz, F.G. Acién-Fernández, A.de F. Iorio, Optimization of the production of lipids and carotenoids in the microalga Golenkinia aff. brevispicula, Algal Res. 51 (2020), 102004, https://doi.org/10.1016/j.algal.2020.102004.
[101] F. De La Coba, J. Aguilera, F.L. Figueroa, M.V. De Gálvez, E. Herrera, Antioxidant activity of mycosporine-like amino acids isolated from three red macroalgae and one marine lichen, J. Appl. Phycol. 21 (2009) 161–169, https://doi.org/10.1007/s10811-008-9345-1.
[102] N. Wada, T. Sakamoto, S. Matsugo, Mycosporine-like amino acids and their derivatives as natural antioxidants, Antioxidants 4 (2015) 603–646, https://doi.org/10.3390/antiox4030603.
[103] R. Mateos, J.R. Pérez-Correa, H. Dominguez, Bioactive properties of marine phenolics, Mar. Drugs 18 (2020) 501, https://doi.org/10.3390/md18100501.
[104] B. Soni, N.P. Visavadiya, D. Madamwar, Attenuation of diabetic complications by C-phycoerythrin in rats: antioxidant activity of C-phycoerythrin including copper-induced lipoprotein and serum oxidation, Br. J. Nutr. 102 (2009) 102–109, https://doi.org/10.1017/S0007114508162973.
[105] N. Senthilkumar, C. Kurinjimalar, R. Thangam, V. Suresh, G. Kavitha, P. Gunasekaran, R. Rengasamy, Further studies and biological activities of macromolecular protein R-Phycoerythrin from Portieria hornemannii, Int. J. Biol. Macromol. 62 (2013) 107–116, https://doi.org/10.1016/j.ijbiomac.2013.08.004.
[106] M. Zubia, D. Robledo, Y. Freile-Pelegrin, Antioxidant activities in tropical marine macroalgae from the Yucatan Peninsula, Mexico, J. Appl. Phycol. 19 (2007) 449–458, https://doi.org/10.1007/s10811-006-9152-5.
[107] C.O. Coura, I.W.F. de Araújo, E.S.O. Vanderlei, J.A.G. Rodrigues, A.L.G. Quinderé, B.P. Fontes, I.N.L. de Queiroz, D.B. de Menezes, M.M. Bezerra, A.A.R. e Silva, H. V. Chaves, R.J.B. Jorge, J.S.A.M. Evangelista, N.M.B. Benevides, Antinociceptive and anti-inflammatory activities of sulphated polysaccharides from the red seaweed Gracilaria cornea, Basic Clin. Pharmacol. Toxicol. 110 (2012) 335–341.
[108] F. Álvarez-Gómez, N. Korbee, F.L. Figueroa, Analysis of antioxidant capacity and bioactive compounds in marine macroalgal and lichenic extracts using different solvents and evaluation methods, Cienc. Mar. 42 (2016) 271–288, https://doi.org/10.7773/cm.v42i4.2677.
[109] P. Algarra, W. Rudiger, Acclimation processes in the light harvesting complex of the red alga Porphyridium purpureum (Bory) Drew et Ross, according to irradiance and nutrient availability, Plant Cell Environ. 16 (1993) 149–159, https://doi.org/10.1111/j.1365-3040.1993.tb00856.x.
[110] R. Aráoz, D.-P. Häder, Ultraviolet radiation induces both degradation and synthesis of phycobilisomes in Nostoc sp.: a spectroscopic and biochemical approach, FEMS Microbiol. Ecol. 23 (1997) 301–313, https://doi.org/10.1111/J.1574-6941.1997.TB00411.X.
[111] N. Tandeau de Marsac, J. Houmard, Adaptation of cyanobacteria to environmental stimuli: new steps towards molecular mechanisms, FEMS Microbiol. Lett. 104 (1993) 119–189, https://doi.org/10.1111/j.1574-6968.1993.tb05866.x.
[112] B.E. Lapointe, C.S. Duke, Biochemical strategies for growth of Gracilaria tikvahiae (rhodophyta) in relation to light intensity and nitrogen availability1, J. Phycol. 20 (1984) 488–495, https://doi.org/10.1111/J.0022-3646.1984.00488.X.
[113] J.J. Vergara, K.T. Bird, F.X. Niell, Nitrogen assimilation following NH4+ pulses in the red alga Gracilariopsis lemaneiformis: Effect on C metabolism, Mar. Ecol. Prog. Ser. 122 (1995) 253–264, https://doi.org/10.3354/meps122253.
[114] A.B. Jones, W.C. Dennison, G.R. Stewart, Macroalgal responses to nitrogen source and availability: amino acid metabolic profiling as a bioindicator using Gracilaria edulis (rhodophyta), J. Phycol. 32 (1996) 757–766, https://doi.org/10.1111/j.0022-3646.1996.00757.x.
[115] L. Talarico, G. Maranzana, Light and adaptive responses in red macroalgae: an overview, J. Photochem. Photobiol. B Biol. 56 (2000) 1–11, https://doi.org/10.1016/S1011-1344(00)00046-4.
[116] J. Beardall, S. Roberts, J. Millhouse, Effects of nitrogen limitation on uptake of inorganic carbon and specific activity of ribulose-1,5-bisphosphate carboxylase/oxygenase in green microalgae 69 (2011) 1146–1150, https://doi.org/10.1139/B91-147.
[117] A. Wulff, K. Sundbäck, C. Nilsson, G.J.C. Underwood, Effects of UVB radiation on a marine microphytobenthic community growing on a sand-substratum under different nutrient conditions, Limnol. Oceanogr. 45 (2000) 1144–1152, https://doi.org/10.4319/LO.2000.45.5.1144.
[118] I. Hernández, A. Corzo, R.J. Gordillo, M. Robles, E. Saez, J. Fernández, R. Niell, Seasonal cycle of the gametophytic form of Porphyra umbilicalis: nitrogen and carbon, Mar. Ecol. Prog. Ser. 99 (1993) 301–311, https://doi.org/10.3354/meps099301.
[119] F. Alvarez-Gomez, Analysis of antioxidant capacity and bioactive compounds in marine macroalgal and lichenic extracts using different solvents and evaluation

methods, Cienc. Mar. 42 (2016) 271–288, https://doi.org/10.7773/cm.v42i4.2677.
[120] H. Taira, S. Taguchi, Cellular Mycosporine-like amino acids protect photosystem II of the Dinoflagellate scrippsiella sweeneyae from ultraviolet radiation damage, J. Photochem. Photobiol. B Biol. 174 (2017) 27–34, https://doi.org/10.1016/J.JPHOTOBIOL.2017.07.015.
[121] F.L. Figueroa, N. Korbee, R. Abdala, C.G. Jerez, M. López-de la Torre, L. Güenaga, M.A. Larrubia, J.L. Gómez-Pinchetti, Biofiltration of fishpond effluents and accumulation of N-compounds (phycobiliproteins and mycosporine-like amino acids) versus C-compounds (polysaccharides) in Hydropuntia cornea (Rhodophyta), Mar. Pollut. Bull. 64 (2012) 310–318, https://doi.org/10.1016/j.marpolbul.2011.11.012.
[122] J.B. Barufi, M.T. Mata, M.C. Oliveira, F.L. Figueroa, Nitrate reduces the negative effect of UV radiation on photosynthesis and pigmentation in Gracilaria tenuistipitata (Rhodophyta): The photoprotection role of mycosporine-like amino acids, Phycologia 51 (2012) 636–648, https://doi.org/10.2216/10.77.1.
[123] B. Briani, M.N. Sissini, L.A. Lucena, M.B. Batista, I.O. Costa, J.M.C. Nunes, C. Schmitz, F. Ramlov, M. Maraschin, N. Korbee, L. Rörig, P.A. Horta, F. L. Figueroa, J.B. Barufi, The influence of environmental features in the content of mycosporine-like amino acids in red marine algae along the Brazilian coast, J. Phycol. 54 (2018) 380–390, https://doi.org/10.1111/jpy.12640.
[124] Y. Sun, N. Zhang, J. Zhou, S. Dong, X. Zhang, L. Guo, G. Guo, Distribution, contents, and types of mycosporine-like amino acids (MAAs) in marine macroalgae and a database for Maas based on these characteristics, Mar. Drugs. 18 (2020) 43, https://doi.org/10.3390/md18010043.
[125] U. Karsten, L.A. Franklin, K. Tüning, C. Wiencke, Natural ultraviolet radiation and photosynthetically active radiation induce formation of mycosporine-like amino acids in the marine macroalga Chondrus crispus (Rhodophyta), Planta 205 (1998) 257–262, https://doi.org/10.1007/s004250050319.
[126] L.A. Franklin, I. Yakovleva, U. Karsten, K. Lüning, Synthesis of mycosporine-like amino acids in Chondrus crispus (florideophyceae) and the consequences for sensitivity to ultraviolet b radiation, J. Phycol. 35 (1999) 682–693, https://doi.org/10.1046/J.1529-8817.1999.3540682.X.
[127] K. Whitehead, J.I. Hedges, Photodegradation and photosensitization of mycosporine-like amino acids, J. Photochem. Photobiol. B Biol. 80 (2005) 115–121, https://doi.org/10.1016/J.JPHOTOBIOL.2005.03.008.
[128] Y. Freile-Pelegrín, D. Robledo, Bioactive phenolic compounds from algae, in: Bioact. Compd. from Mar. Foods Plant Anim. Sources, Wiley Blackwell, 2013, pp. 113–129, https://doi.org/10.1002/9781118412893.ch6.
[129] P.S.M. Celis-Plá, M.T. Brown, A. Santillán-Sarmiento, N. Korbee, C.A. Sáez, F. L. Figueroa, Ecophysiological and metabolic responses to interactive exposure to nutrients and copper excess in the brown macroalga Cystoseira tamariscifolia, Mar. Pollut. Bull. 128 (2018) 214–222, https://doi.org/10.1016/J.MARPOLBUL.2018.01.005.
[130] Y. Freile-Pelegrín, Does storage time influence yield and agar properties in the tropical Agarophyte Gracilaria cornea? J. Appl. Phycol. 12 (2000) 153–158, https://doi.org/10.1023/A:1008150524093.
[131] J. Orduña-Rojas, D. Robledo, Studies on the tropical agarophyte Gracilaria cornea J. Agardh (Rhodophyta, Gracilariales) from Yucatán, México. II. Biomass assessment and reproductive phenology, Bot. Mar. 45 (2002) 459–464, https://doi.org/10.1515/BOT.2002.047/MACHINEREADABLECITATION/RIS.
[132] A. Neori, I. Cohen, H. Gordin, Ulva lactuca biofilters for marine fishpond effluents II. Growth rate, yield and C:N ratio, Bot. Mar. 34 (1991) 483–490, https://doi.org/10.1515/botm.1991.34.6.483.
[133] S. Andayani, R. Yuwanita, N. Izzah, Biofilter application using seaweed (Gracillaria verucosa) to increase production of Vannameii shrimp in traditional pond district Bangil-Pasuruan, Res. J. Life Sci. 3 (2016) 16–22, https://doi.org/10.21776/UB.RJLS.2016.003.01.3.
[134] F. de la Coba, J. Aguilera, N. Korbee, M.V. de Gálvez, E. Herrera-Ceballos, F. Álvarez-Gómez, F.L. Figueroa, UVA and UVB Photoprotective capabilities of topical formulations containing mycosporine-like amino acids (maas) through different biological effective protection factors (BEPFs), Mar. Drugs 17 (2019), https://doi.org/10.3390/md17010055.
[135] A. Torres, C.D. Enk, M. Hochberg, M. Srebnik, Porphyra-334, a potential natural source for UVA protective sunscreens, Photochem. Photobiol. Sci. 5 (2006) 432–435, https://doi.org/10.1039/b517330m.
[136] J. Ryu, S.J. Park, I.H. Kim, Y.H. Choi, T.J. Nam, Protective effect of porphyra-334 on UVA-induced photoaging in human skin fibroblasts, Int. J. Mol. Med. 34 (2014) 796–803, https://doi.org/10.3892/ijmm.2014.1815.
[137] A. Hartmann, J. Gostner, J.E. Fuchs, E. Chaita, N. Aligiannis, L. Skaltsounis, M. Ganzera, Inhibition of collagenase by mycosporine-like amino acids from marine sources, Planta Med. 81 (2015) 813–820, https://doi.org/10.1055/s-0035-1546105.
[138] K. Becker, A. Hartmann, M. Ganzera, D. Fuchs, J. Gostner, Immunomodulatory effects of the mycosporine-like amino acids shinorine and porphyra-334, Mar. Drugs 14 (2016) 119, https://doi.org/10.3390/md14060119.
[139] E. Chrapusta, A. Kaminski, K. Duchnik, B. Bober, M. Adamski, J. Bialczyk, Mycosporine-Like Amino Acids: Potential Health and Beauty Ingredients, Mar. Drugs 15 (2017) 326, https://doi.org/10.3390/md15100326.
[140] K.P. Lawrence, P.F. Long, A.R. Young, Mycosporine-like amino acids for skin photoprotection, Curr. Med. Chem. 25 (2017) 5512–5527, https://doi.org/10.2174/0929867324666170529124237.